PLANE WAVE SPECTRUM ANALYSIS OF NEAR-ZONE FIELDS USING WAVENUMBER BAND-PASS FILTERING

A THESIS

Presented to

The Faculty of the Division of Graduate Studies

By

Everette Clifton Burdette II

In Partial Fulfillment

of the Requirements for the Degree

Master of Science

in the School of Electrical Engineering

Georgia Institute of Technology

May 1976

PLANE WAVE SPECTRUM ANALYSIS OF NEAR-ZONE FIELDS

USING WAVENUMBER BAND-PASS FILTERING

APPROVED:

John D. Norgard, Chairman

W. Marshall Leach, Jr.

Charles E. Ryan, Jr.

Date approved by Chairman 21 May 1976

ACKNOWLEDGMENTS

The preparation of any thesis involves the efforts of many people besides the author. I take this opportunity to express my sincere gratitude to those who have made the successful completion of this study possible.

First, I thank my thesis advisor, Dr. John D. Norgard, whose contributions have been numerous. His many suggestions, criticisms, and kind devotion of his time have been instrumental in the successful completion of this thesis. Special thanks also go to Dr. W. Marshall Leach, Jr., who served on the reading committee, for his suggestions and contributions to the quasi-optical development.

The thesis was read in its initial form by my teacher, friend, and colleague, Dr. Charles E. Ryan, Jr., who served on the reading committee and has been a constant source of advice and help. The idea to study wavenumber bandpass filtering techniques was originally his, and his interest and guidance have been extremely helpful throughout the preparation of this thesis. As has been the case since I first met him, I have profited from his kind and careful consideration.

Special acknowledgment is also made to Dr. H. Allen Ecker, Mr. Fred L. Cain, and Dr. J. Lee Edwards for their administrative support which made this study possible. Further, I express my deep appreciation to Mr. Cain for his constant encouragement and moral support. Thanks are also due to Mrs. Peggy Weldon and Ms. Janet Meredith for their skillful typing of the manuscript.

Finally, I would like to thank my loving wife, Sheila, for her kind and patient understanding during often very trying conditions. Her encouragement has been an essential ingredient in the writing of this thesis.

TABLE OF CONTENTS

LIST OF TABLES

LIST OF ILLUSTRATIONS

LIST OF ILLUSTRATIONS (Continued)

LIST OF ILLUSTRATIONS (Continued)

LIST OF ILLUSTRATIONS (Continued)

SUMMARY

The objective of this thesis was to examine a criterion for determining the number of spectral samples required to describe the significant field contributions in a particular near-field region and for determining the location of the region in wavenumber space. The employment of such a "wavenumber band-pass filtering" criterion for either measured or theoretical near-field distributions is particularly useful for determining the local field incident upon a scatterer located in the near field of a radiating structure or for determining potential radiation hazards occurring in limited near-field sectors of radar antennas.

Many near-field analyses of microwave antennas have been based on the Green's function solution of the wave equation in which the near fields are computed by direct integration of the aperture fields. However, recently other methods of analysis have been employed. It is a well known fact that it is possible to represent an arbitrary electromagnetic field as a superposition of plane waves. Techniques utilizing the Plane Wave Spectrum (PWS) analysis recently developed are very flexible and offer a great amount of information about the nature of an electromagnetic field on a plane near an antenna. The PWS method for the computation of the antenna near-zone fields is significantly faster than the aperture field integration method for near-field analyses of large antennas, and by bandpass filtering the PWS in wavenumber space, a method of analysis of antennas is developed here which is faster than

both the original PWS method and the aperture field method. Once the near field on a plane in front of the antenna is known either by measurement or calculation, wavenumber bandpass filtering may be employed to minimize the number of spectral samples required to accurately compute the near field of an antenna over a particular angular sector at any farther-out near-field distance.

The plane wave spectrum of an antenna takes the form of a two-dimensional Fourier transform of the electromagnetic field. As the plane wave spectrum obtained is directly related to the far-field radiation pattern of the antenna, a Fourier transform relationship is seen to exist between the two-dimensional near field and the radiated far field. At infinity, the field may be represented by a single plane wave. However, at close-in near-field distances, the PWS integral expression formally requires integration over all wavenumber space. It has been determined that for non-supergain antennas, integration need only be performed over the wavenumbers which contribute to the radiated field. The wavenumbers outside the visible (radiated) wavenumber region represent evanescent waves which attenuate very rapidly with increasing distance for non-supergain antennas. Evan at distances as small as a few wavelengths from the radiating structure. The evanescent waves have attenuated such that only plane waves which correspond to the radiated (visible) wavenumber region have a significant contribution to the near-zone fields.

Presented in this thesis is a method for further wavenumber limiting which utilizes only those spectral components which make significant contributions to the field. At distances of a few wavelengths from an

antenna, the region which adequately describes the significant contributions to the field includes all visible wavenumbers. As the distance from the antenna is increased, the required size of this region decreases until at large distances (far field) only the wavenumber corresponding to the angular direction of the field point of interest is required. Therefore, in most cases integration over all visible wavenumbers is not required to adequately describe the near field of a radiating structure. Further, this fact can be applied for cases where the near-field region of interest for a particular antenna occupies only a small sector of the total near field to significantly reduce the size of the wavenumber region required for accurate description of the field. This is true even for close-in distances which would normally require integration over a larger wavenumber region. Therefore, the PWS of an antenna or scatterer can be bandpass filtered to include only those wavenumber samples necessary to describe the near-field sector of interest, resulting in substantial savings in computer time and storage requirements. In this thesis, a technique is developed for determining the size of the wavenumber region needed to adequately describe the antenna near field in a particular location and where that region should be located in wavenumber space.

This technique has been verified by comparing near-zone radiation patterns computed from wavenumber bandpass filtered spectral data to (1) near-zone patterns computed from unfiltered spectral data and (2) near-zone patterns computed using aperture integration techniques. For each case, a comparison of data requirements and computation time has been performed. The results indicate that this is an efficient technique for the near-field analysis of many aperture antennas.

CHAPTER I

INTRODUCTION

Brief History of Near Field Analysis Techniques

The analysis of aperture near-field distributions has been of major interest to antenna researchers for many years. Considerable effort has been devoted to the analysis and calculation of antenna near fields. Commonly used analyses have been based on the Green's function solution [1] of the wave equation. Summaries and discussions of the various approaches are given by Hansen [2]. Most of the near-field analyses have been based on relatively simple models using the Kirchoff formulation [2,3], such an aperture in an infinite plane. For example, parabolic dish antennas have been modelled in this manner where the aperture plane contained the rim of the reflector where according to the Kirchoff assumptions, fields were nonzero in the forward region and zero in geometric shadow regions. Often, for cases of circular and rectangular apertures, theoretical aperture illumination functions were used for the analyses [3-5]. Significant effort has been directed to the development of numerical techniques for utilization of the approaches described by Bouwkamp [3], Hansen [2], and Jacobs [6]. Fresnel and Fraunhofer approximations were employed in these numerical analyses in order to simplify the integral formulation, resulting in Fresnel integrals for which solutions were readily obtainable. However, these approximations did not necessarily result in adequate representation of real antennas.

The Fresnel approximation applied to the exact integral formulation restricted the validity of these expressions to near-field regions having small angular displacement from the boresight axis. Also, a large amount of time was required to compute these integrals for relatively large apertures.

Most near-field analyses to date have employed the direct aperture field integration method discussed above. However, Plane Wave Spectrum (PWS) theory provides another approach for near-field analysis. Booker and Clemmow [7] derived a formulation using the angular spectrum of plane waves. The approach was later extended to the three-dimensional case by Brown [8]. Although this formulation has existed for many years, only recently has this approach been used for near-field calculations. The PWS representation of an arbitrary electromagnetic field [9] is used to represent the propagating EM field as a summation of individual plane waves which propagate in different spatial directions. The development of the Fast Fourier Transform algorithm and more recently, advanced measurement techniques [10,11], has permitted far and near zone radiation properties of an antenna to be efficiently derived from either a theoretical aperture distribution or near-field measurements.

The determination of far-field antenna radiation patterns from near-field measurements has recently been a topic of wide interest [12-14]. During the last few years, several investigations have resulted in the development of measurement techniques [14-17] which utilized measured amplitude and phase data for the calculation of far-zone antenna radiation patterns rather than an assumed aperture distribution. Joy and Paris [10] have derived relationships between the antenna and probe

separation distance, evanescent wave attenuation, and the required sample spacing. Leach [11] extended these techniques to cylindrical coordinates by deriving the cylindrical wave expansion of the EM field radiated by an antenna and determining the required spatial sampling. In each case, the spectrum approach was used and these techniques are summarized in a paper by Johnson and Ecker [18].

In the computation of near-field patterns either aperture integration or PWS techniques may be used. However, for large apertures a considerable amount of computer time is required to compute the near fields because a time consuming numerical integration is required rather than the rapid Fast Fourier Transform algorithm. However, Rudduck et al. [19] computed the near fields utilizing the PWS approach. Although at close-in near-field distances the PWS integral formally requires integration over all wavenumber space, Rudduck et al. [19] determined that in many cases integration is required only over the visible wavenumber spectrum (i.e., wavenumbers corresponding to radiated waves). This agrees with Rhodes' [20] statement that wavenumbers outside the visible wavenumber region represent evanescent waves which are associated with determining the reactive impedance of an antenna and therefore, do not contribute to the radiated field. The result is that fewer integration points are required for the PWS method than for the aperture field integration method. In addition to the reduction in required integration points, a significant reduction in computation time could also be achieved. The reduction in computation time afforded by the PWS technique is greatest for close-in near-field distances. In the close near-field region, Fresnel approximations are not valid and the computation time for the aperture integration

method is proportional to the square of the aperture size. However, PWS computation times are approximately linearly proportional to aperture size for close-in distances. Therefore, the PWS method is considerably faster at close-in near-field distances, especially for large apertures.

This fact has been further exploited by Brown [21] in determining the near fields of large circular apertures. It was determined that even further savings in computer time could be accomplished by integration over only those wavenumbers which contained all significant contributions to the field. However, this analysis lacked an analytical approach by which the size and location of the required wavenumber region could be determined for a particular spatial sector of interest. To date, the only method employed to determine the required size and approximate location of the wavenumber region was to integrate over several increasingly larger wavenumber regions until convergence was obtained.

Purpose of this Research

The purpose of this research is to further develop the plane wave spectrum analysis technique for determination of antenna near-zone radiation patterns. This overall objective is met through three specific objectives.

First, an efficient numerical integration technique is chosen which overcomes the limitations of the discrete Fast Fourier Transform. A Bivariate integration rule which interpolates between the sampled data points is useful for this application. This quadrature rule employs a linear interpolation to approximate the value of the integrand in the

intervals between the sampled data points, thus providing a means for approximating a continuum of spectra over the range of spectral samples.

Second, a criterion for determining the size of the spectral region required to accurately describe the antenna near field in a particular angular sector is examined based on a quasi-optical approximation.

Third, a technique to determine the location of the spectral region used to describe the antenna near field at a particular observation angle is developed based on the principle of stationary phase.

The Bivariate integration rule and bandpass filtering techniques are then employed in near-field PWS computations to demonstrate their usefulness in near-field analyses.

CHAPTER II

ANALYTICAL FORMULATION

In this chapter, the analytical background for the problem of determining the near field of an antenna over a particular region of interest using wavenumber bandpass filtering is developed. It is shown that the plane wave spectrum of the radiated field can be determined from a knowledge of the transverse field components over a plane directly in front of the antenna. Methods for determining the near-zone fields of an antenna are then discussed and a quasi-optical technique for determining the size of the spectral region required to accurately describe a particular near-field sector and its angular location is developed. Finally, a method is presented to verify that the quasi-optical technique satisfies the uncertainty principle.

Plane Wave Spectrum Representation of Electromagnetic Fields

The basic EM problem is to satisfy the vector Helmholtz wave equation subject to the boundary conditions of the EM fields. The Plane Wave Spectrum representation of electromagnetic fields can be used to accomplish this goal in the following manner. As previously noted, the electromagnetic field can be represented as a superposition of plane waves, all of the same frequency, propagating in different directions with different amplitudes. The electric field of each of the plane waves has the form

$$\bar{E}(x,y,z,t) = \bar{\bar{A}}(\bar{k})e^{j(\omega t - \bar{k} \cdot \bar{r})} , \qquad (1)$$

where $\bar{\bar{A}}(\bar{k})$ are the plane wave spectra of the field,

r is the radius vector to the field point,

ω is the angular frequency, and

$\bar{k}$ is the vector wavenumber = $\hat{n}(\frac{2\pi}{\lambda})$ where $\hat{n}$ is a unit vector in the direction of propagation.

The radius vector to the point (x,y,z) is defined to be

$$\bar{r} = x\hat{x} + y\hat{y} + z\hat{z} . \qquad (2)$$

The vector wavenumber $\bar{k}$ expressed in rectangular coordinates is

$$\bar{k} = k_x\hat{x} + k_y\hat{y} + k_z\hat{z} = \hat{n}\,k_o \qquad (3)$$

$\hat{x}$, $\hat{y}$, and $\hat{z}$ are the unit vectors of the (x,y,z) cartesian coordinate set shown in Figure 1. In this analysis, only near fields on some planar surface in front of the radiating surface are of interest. Therefore, the antenna (or scatterer) itself is excluded from the region of analysis by an aperture plane as shown in Figure 2. Each of the plane waves in the spectra which comprise the total field must satisfy the wave equation

$$\nabla^2 \bar{E}(x,y,z,t) - (\frac{2\pi}{\lambda})\,\bar{E}(x,y,z,t) = 0 , \qquad (4)$$

where λ is the free space wavelength and ∇^2 is the Laplacian in rectilinear coordinates. The solution of this wave equation is subject to the following set of boundary conditions:

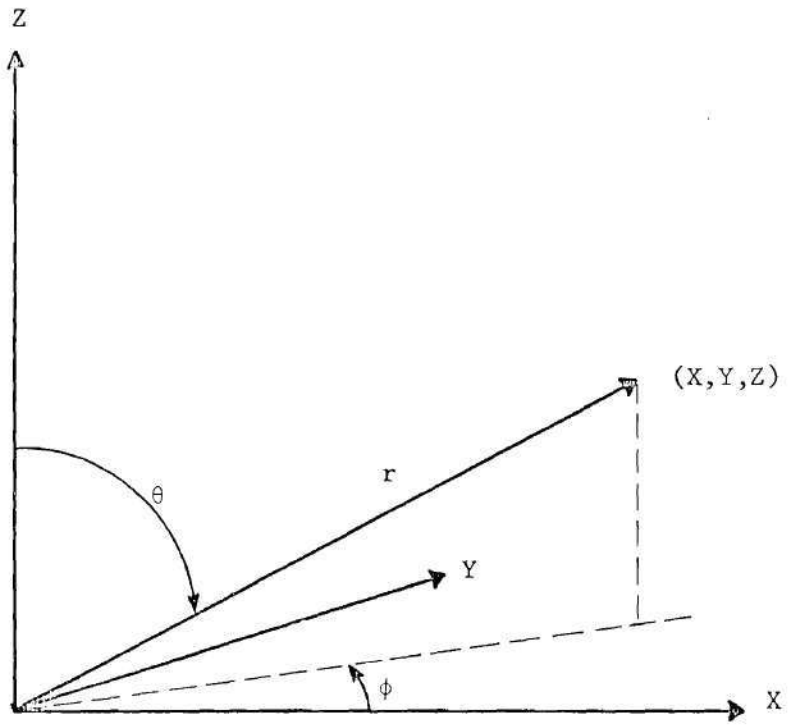

Figure 1. Coordinate System

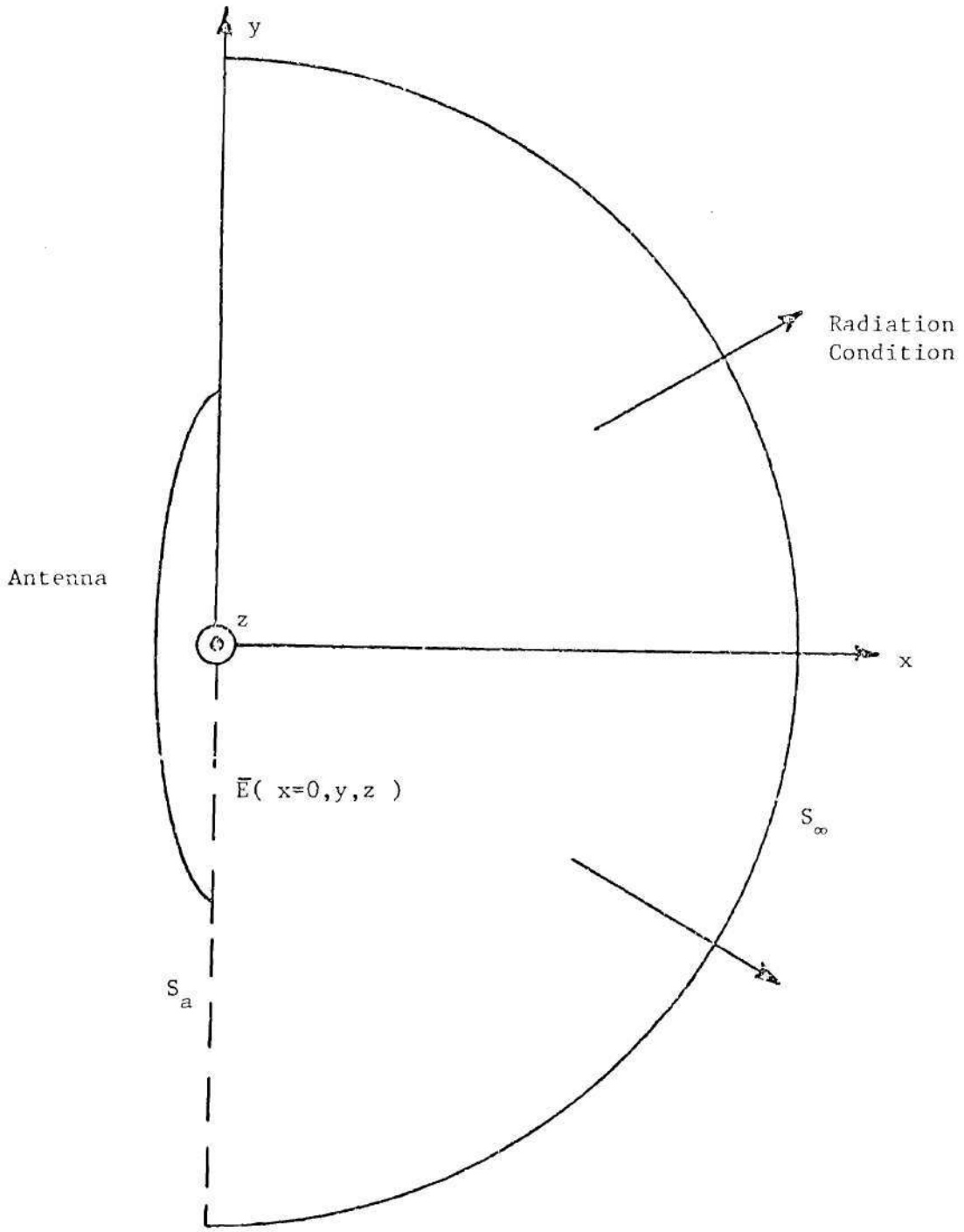

Figure 2. Diagram of the Aperture Plane Employed in the Plane Wave Spectrum Representation of the Antenna and the Surface at Infinity Where the Electromagnetic Field Must Satisfy the Radiation Condition.

$$1.\quad \bar{E}(0,y,z) = \bar{E}_o(y,z)\ ,$$

$$2.\quad \lim_{r\to\infty}\left(jkE - \frac{\partial E}{\partial r}\right) = 0, \text{ and} \tag{5}$$

$$3.\quad \nabla \cdot \bar{E} = 0.$$

The first boundary condition is the specification of the measured or assumed fields on the x = 0 plane in front of the antenna. The second boundary condition is the radiation condition at infinity. Since the radiation occurs in an unbounded charge-free region, the third boundary condition is introduced by Poisson's equation, which physically means that it is only necessary to know any two of the three spatial field components [9]. It is therefore sufficient to measure only the transverse field components, i.e., the field components lying in the plane orthogonal to the x-axis.

Substituting the plane wave expression, Equation (1), into the wave equation, Equation (4), results in the following restriction on the vector wavenumber $\bar{k}$

$$k_x^2 + k_y^2 + k_z^2 = (2\pi/\lambda)^2 = k_o^2\ . \tag{6}$$

The rectangular components of the vector wavenumber $\bar{k}$, with magnitude k_o, may also be expressed in terms of the angles θ and ϕ of Figure 1 as

$$k_x = k_o \sin\theta \cos\phi\ ,$$

$$k_y = k_o \sin\theta \sin\phi\ , \text{ and} \tag{7}$$

$$k_z = k_o \cos\theta\ .$$

The solution of the wave equation may be determined either by using the Green's function method or by using the Fourier transform method. In the Green's function method, the field is expressed in terms of the aperture field. The Fourier transform method leads to solutions expressed in terms of the plane wave spectrum. The vector $\bar{A}$ in Equation (1) is a function of the propagation direction $\bar{k}$. If the direction of propagation is known, only two of the vector components of $\bar{A}$ are required to specify its orientation because the third component is uniquely determined by Poisson's constraint equation, listed as third in Equation (5). Therefore, the complex vector $\bar{A}(k_y,k_z)$ is taken as the plane wave spectra of the transverse aperture field components. If the tangential electric field $\bar{E}_t(0,y,z)$ is known over the x = 0 plane, $\bar{A}(k_y,k_z)$ can be determined from [9-11]

$$\bar{E}_t(0,y,z) = \frac{1}{2\pi} \int_{-\infty}^{\infty} \int_{-\infty}^{\infty} \bar{A}(k_y,k_z) e^{-j(k_y y + k_z z)} dk_y dk_z . \qquad (8)$$

Thus $\bar{A}(k_y,k_z)$ is related, by a Fourier transform pair, to the transverse field components over the x = 0 plane, as

$$\bar{A}(k_y,k_z) = \frac{1}{2\pi} \int_{-\infty}^{\infty} \int_{-\infty}^{\infty} \bar{E}_t(0,y,z) e^{j(k_y y + k_z z)} dydz , \qquad (9)$$

where the x = 0 plane is the plane on which the field components are known and the $e^{j\omega t}$ time dependence has been suppressed. The field may also be reconstructed at a near-field plane other than the plane on which the field components were originally known. To obtain the field at any near-field distance in terms of $\bar{A}(k_y,k_z)$ at the x = 0 plane, the inverse

Fourier relationship is employed to give [9-11],

$$\bar{E}(x,y,z) = \frac{1}{2\pi} \int_{-\infty}^{\infty} \int_{-\infty}^{\infty} \bar{A}(k_y,k_z) e^{-j[k_x(k_y,k_z)x+k_y y+k_z z]} dk_y dk_z \quad (10)$$

where $k_x(k_y,k_z) = \sqrt{k_o^2 - k_y^2 - k_z^2}$. In general, this integral is difficult to evaluate, but as the distance in terms of the radius vector $\bar{r}$ to the field point approaches infinity, the method of stationary phase [22] may be employed to evaluate the integral analytically. By transforming from rectangular coordinates to spherical coordinates and then applying the stationary phase principle, the far-field at range $r > 2D^2/\lambda$, where D is the maximum antenna dimension is given by [9],

$$\bar{E}(r,\theta,\phi) = \frac{-je^{-jk_o r}}{r} k_x \bar{A}(k_y,k_z) , \quad (11)$$

where (r,θ,ϕ) is the far-field observation point which has a one-to-one correspondence to a point in wavenumber space. That is, at infinity the wavenumber bandwidth is just a single point which is equivalent to saying that the field at infinity is described by a single plane wave. This is true for all $k_y^2 + k_z^2 \leq k_o^2$ which correspond to all real angles of propagation. For these wavenumbers, the propagation constant in the x-direction is given by

$$k_x = + \sqrt{k_o^2 - k_y^2 = k_z^2} , \quad (12)$$

where the positive sign on the radical indicates propagation away from the antenna or scatterer. Wavenumbers having a real propagation constant (i.e., the imaginary part of the complex propagation constant is

zero) propagate without attenuation. Wavenumbers having coordinates such that $k_y^2 + k_z^2 > k_o^2$ and are outside of the visible region shown in Figure 3 correspond to complex angles of propagation and imaginary k_x given by

$$k_x = -j \sqrt{k_y^2 + k_z^2 - k_o^2} , \tag{13}$$

where the negative sign is chosen to ensure that these evanescent waves attenuate in the propagation direction away from the source. In the majority of practical cases, even in the near field, it is not necessary to use the spectral components that correspond to the evanescent waves to compute the field. Thus all of the wavenumber spectral components which lie outside of the visible wavenumber (k_o) circle can usually be neglected.

In the case where the aperture field $\overline{E}_t(0,y,z)$ is known either by specifying the field or by measuring the field of an operating antenna at a number of points in the aperture, a two-dimensional discrete Fast Fourier Transformation (FFT) can be employed to compute the spectrum $\overline{A}(k_y,k_z)$ expressed by Equation (9). If the antenna aperture distribution is known, an analytical expression can be used to compute the field at an array of points; however, if the aperture distribution is not known, a near-field measurement can be performed by scanning a measurement probe in a plane parallel to the antenna aperture and by sampling the amplitude and phase at a discrete number of points on that plane. This measurement is repeated for two orthogonal orientations of the probe so that two orthogonal components of $\overline{E}_t(0,y,z)$ can be determined.

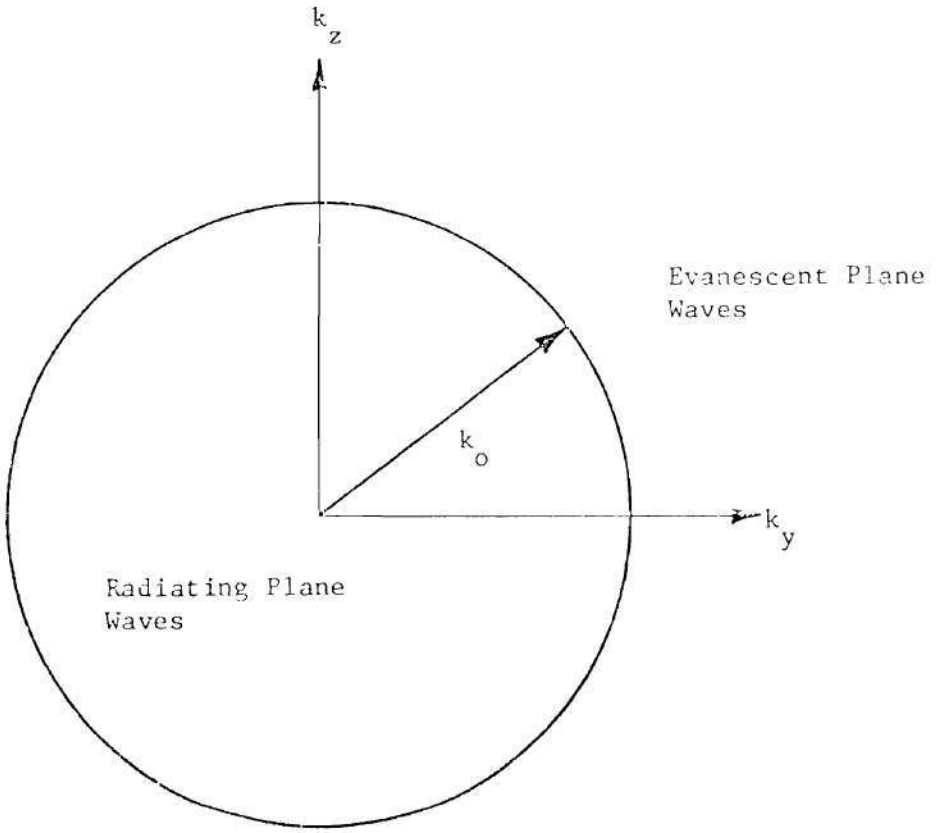

Figure 3. The Free Space Wavenumber (k_o) Boundary Between the Radiating (i.e., Visible) and Evanescent (i.e., Invisible) Wavenumber Regions.

The near-field measurement technique for determining the fields of an operating antenna requires knowledge of the following:

1. the sample spacing required for an accurate determination of the antenna spectrum $\bar{A}(k_y,k_z)$ and
2. the effect of the measurement probe on the determination of the antenna spectrum $\bar{A}(k_y,k_z)$.

Joy and Paris [10] have derived the relationships between the antenna to probe distance, the evanescent wave attenuation, and the required sample spacing. In practice, it has been found that a sample spacing of less than the Nyquist criteria of one-half wavelength is necessary and sufficient for obtaining accurate far-field pattern results. Kerns [23] has shown that the effects of the measurement probe on the measured near-field distribution can be corrected for by use of the Lorentz reciprocity principle. To make the correction requires that the spectrum of the probe antenna (i.e., its far-field pattern) be known in polarization, amplitude, and phase. If this information is available by either measurement or theory, the effects of the probe can be removed by computation.

Figure 4 shows the square grid of NxN sample points which are processed by the discrete FFT, and Figure 5 illustrates how an arbitrary antenna aperture distribution can be located within this square grid. In the case of measured data, the fields outside the aperture are not identically zero. However, the measurement is usually made over a large dynamic range, typically -50 dB to -60 dB, and the fields outside the measurement aperture which are less than that amplitude are neglected.

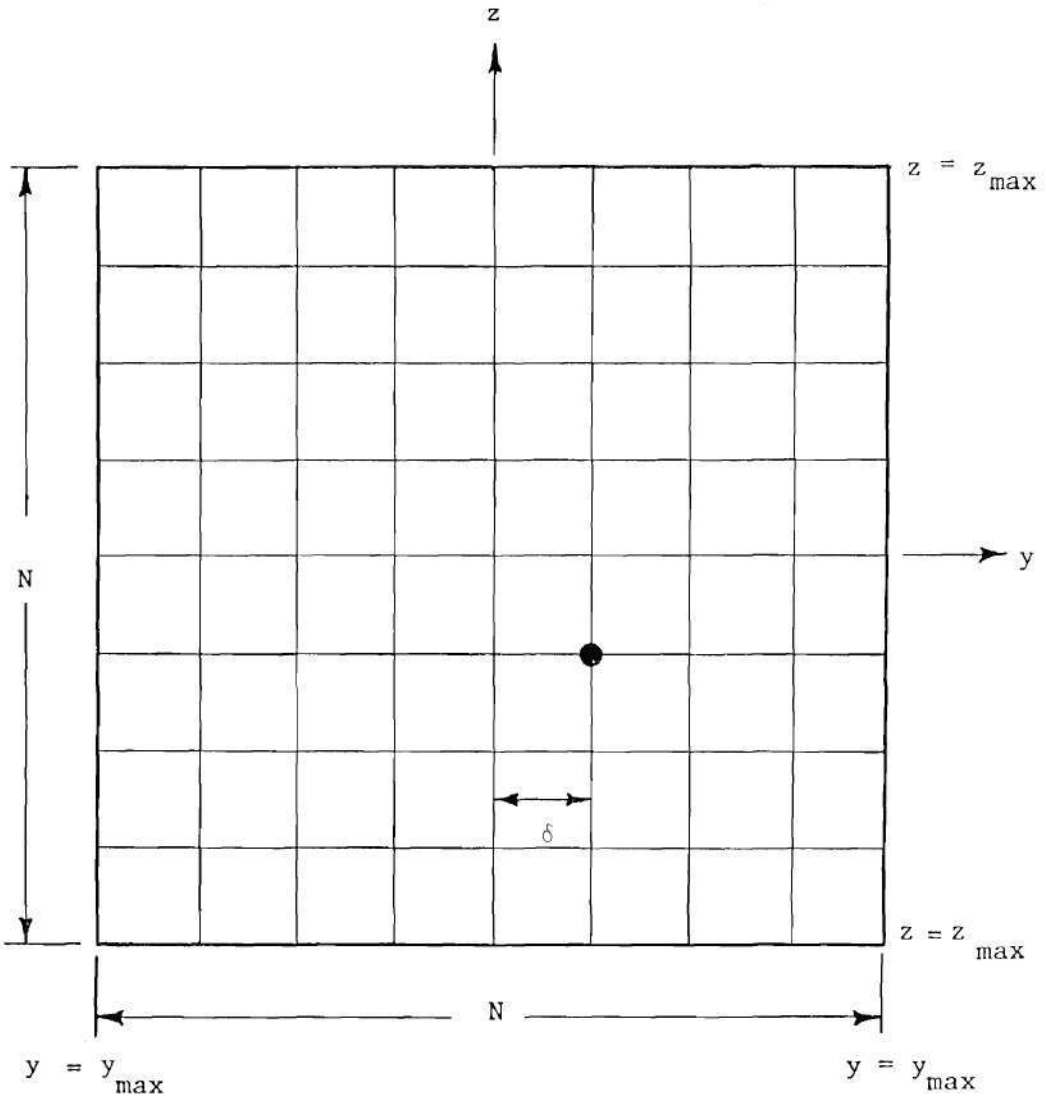

Figure 4. A Square Array of N x N Sample Points Separated by the Distance δ, Where the Aperture Field at Each Sample Point is to be Specified for FFT Processing.

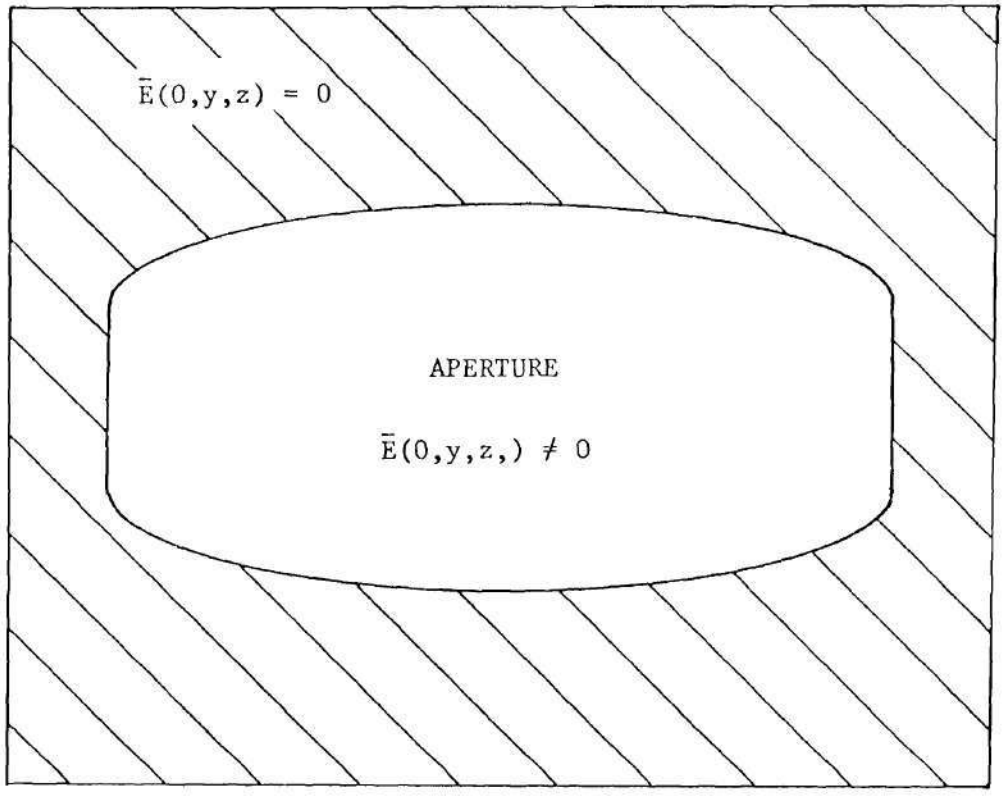

Figure 5. A Pictorial View of the Procedure for Representing an Arbitrary Aperture Shape by Specifying a Zero Aperture Field in the Data Array Outside the Aperture Boundary.

This effectively replaces the infinite limits on the integral for the spectrum $\bar{A}(k_y,k_z)$ (Equation 9) by maximum limits $\pm y_{max}$ and $\pm z_{max}$.

Determination of Near-Zone Fields

In contrast to the relatively straightforward application of the Fourier transformation to compute the far-zone antenna fields, the near-zone fields are more difficult to determine. Usually these near fields are computed by a direct integration of the aperture fields using either a scalar or vector formulation [1,24]. However, it has been shown by Rudduck et al. [19] that a PWS formulation for the computation of antenna near fields can result in a significant reduction in computation time with respect to an aperture integration technique for the case of circularly symmetric aperture distributions.

The direct application of the FFT algorithm to the determination of the near fields from the PWS integral

$$\bar{E}(x,y,z) = \frac{1}{2\pi} \int_{-k_{z(max)}}^{k_{z(max)}} \int_{-k_{y(max)}}^{k_{y(max)}} \bar{A}(k_y,k_z) e^{-j[k_x(k_y,k_z)x+k_y y+k_z z]} dk_y dk_z, \tag{14}$$

with $k_x(k_y,k_z) = \sqrt{k_o^2 - k_y^2 - k_z^2}$ and $x > 0$,

encounters computational problems if the fields over a large angular sector of the near-field region are to be determined. This is due to a fundamental limitation on discrete FFT processing to calculate antenna near fields which will be discussed in the following chapter. Because of this limitation, the integral of Equation (14) must in general be computed using a numerical quadrature formula which causes a significant increase in the required computation time compared to FFT processing.

However, this numerical quadrature can be made very efficient using a bandpass filtering technique which is presented here. This method utilizes in the computation only those spectral components which make significant contributions to the field in the spatial region of interest. At distances of a few wavelengths from an antenna, the wavenumber region which adequately describes the significant contributions to the field includes all visible wavenumbers. As the distance from the antenna is increased, the required size of this region decreases until at large distances (far-field), only the wavenumber corresponding to the angular direction of the field point of interest is required. Therefore, in most cases, integration over all visible wavenumbers is not required to adequately describe the near field of a radiating structure. Further, this fact can be applied for cases where the near-field region of interest for a particular antenna or scatterer occupies only a small sector of the total near field to significantly reduce the size of the wavenumber region and therefore, computation time required for accurate description of the field. This fact is true even for close-in near-field distances that would presumably require integration over a large wavenumber region. Therefore, the PWS of an antenna or scatterer can be "bandpass filtered" to include only those wavenumbers necessary to describe the near-field sector of interest. Consider that the near field on a plane in front of an antenna is known either by measurement or computation using the known and complete visible wavenumber spectrum. From this, one may employ wavenumber bandpass filtering to determine the size of the wavenumber region needed to adequately describe a particular

near-field sector at any farther-out near-field distance and where that region should be located in the wavenumber space.

In the following subsection, these techniques are formulated, and methods are presented which allow the predetermination of the necessary band-limited wave spectrum set. Also, the use of the bandpass filtered PWS method for near-field pattern predictions based upon a quasi-optical technique for mapping the desired angular sector into wavenumber space is discussed.

Wavenumber Bandpass Filtering

In order to compute the antenna near field using the plane wave spectrum $\overline{A}(k_y,k_z)$, the integral

$$\overline{E}(x,y,z) = \frac{1}{2\pi} \int_{-k_{z(max)}}^{k_{z(max)}} \int_{-k_{y(max)}}^{k_{y(max)}} \overline{F}(k_y,k_z,x) e^{-j[k_y y + k_z z]} dk_y dk_z, \qquad (15)$$

where

$$\overline{F}(k_y,k_z,x) = \overline{A}(k_y,k_z) e^{-jx\sqrt{k_o^2 - k_y^2 - k_z^2}} .$$

must be evaluated.

For the far-field case ($x \to \infty$), this integral can be evaluated using the principle of stationary phase, resulting in the expression given by Equation (11), and as a result each far-field direction corresponds to a single plane-wave spectrum component. However, in the near field a large number of the plane-wave spectrum components can contribute to the evaluation of the integral expression given by Equation (15).

The PWS region which contributes to the evaluation of the integral is determined by the behavior of the phase term of the integral given by

$$\phi(k_y,k_z) = (k_y y + k_z z + \sqrt{k_o^2 + k_y^2 + k_z^2}\ x) \ . \qquad (16)$$

If this phase term is slowly varying, i.e., it is stationary, and the phase of $\bar{A}(k_y,k_z)$ is also slowly varying, a net contribution to the integral results since the total integrand is then slowly varying. If this phase term is rapidly varying, the phase of the integrand varies rapidly producing rapid alternate positive and negative oscillations of the integrand which result in no net contribution to the integral. Therefore, although a region of the PWS results in a significant contribution to the antenna field, the spectrum components outside that region yield no net contribution to the integral and do not contribute to the antenna near field.

This phenomenon can be illustrated by examining the behavior of the phase term given by Equation (16), as a function of the near-field location specified by (x,y,z). Figure 6 shows a computer generated phase map for the near-field location x = 20, y = 0, z = 0 cm. Note the relatively large constant phase region at the center of the spectrum $k_y = k_z = 0$ which is the stationary phase point. When the x distance (away from the source) is increased to 100 cm, the phase map shown in Figure 7 results where the stationary phase point remains at $k_y = k_z = 0$, but the phase oscillations due to k_y and k_z are more rapid due to the $k_x x$ term in Equation (16). Further, when the near-field position is moved off the boresight (y = z = 0) direction to the location x = 40, y = 5, z = 5 cm,

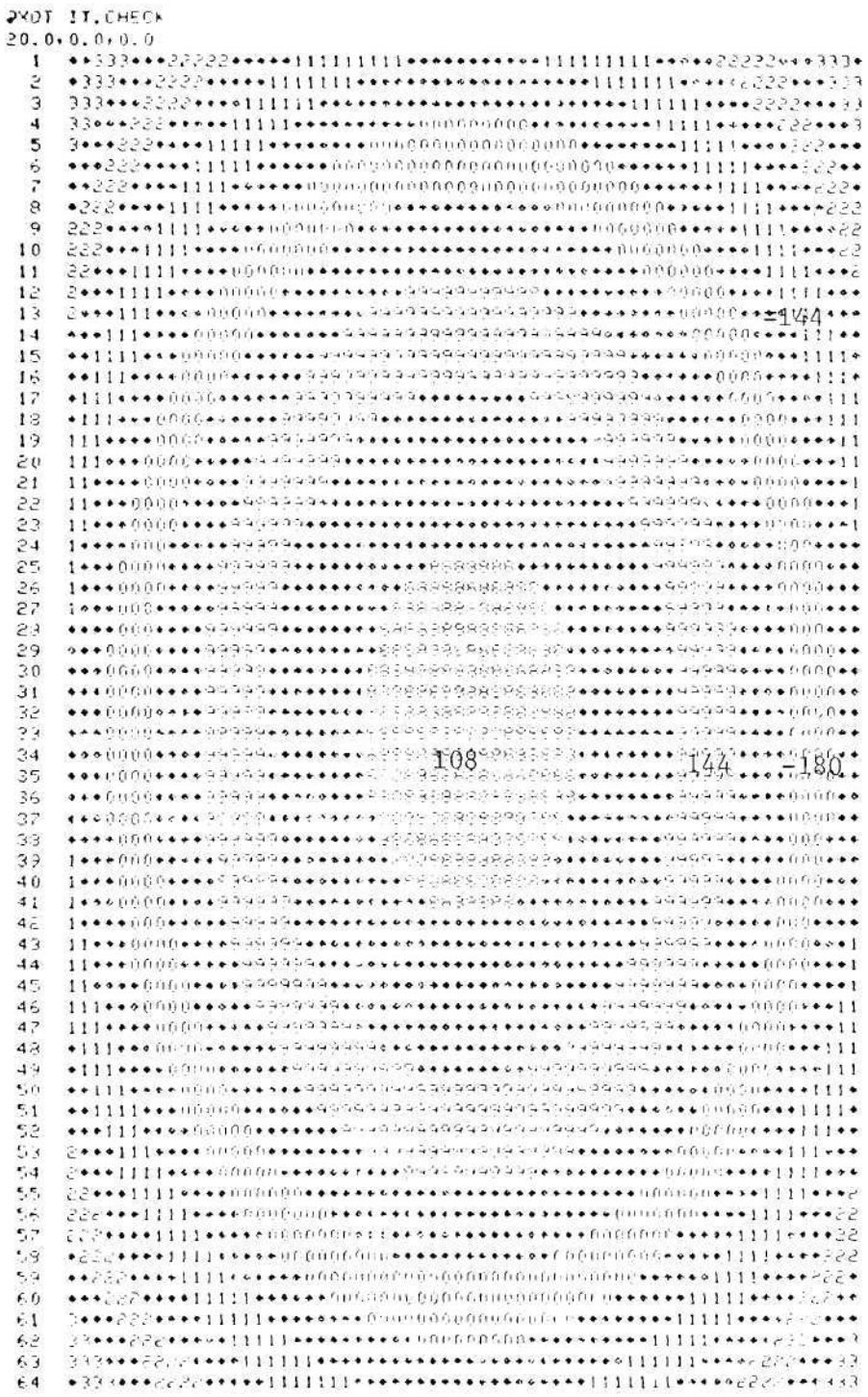

Figure 6. A Computer Generated Phase Map of a Uniform Phase and Amplitude Plane Wave Spectrum that Has Been Shifted to a New Location in Space, i.e., x = 20, y = 0 cm. This Phase Map Represents the Phase Variation Over a ±20° Angular Sector. (The Scale of 0 to 10 Corresponds to a Range of -180° to +180°.)

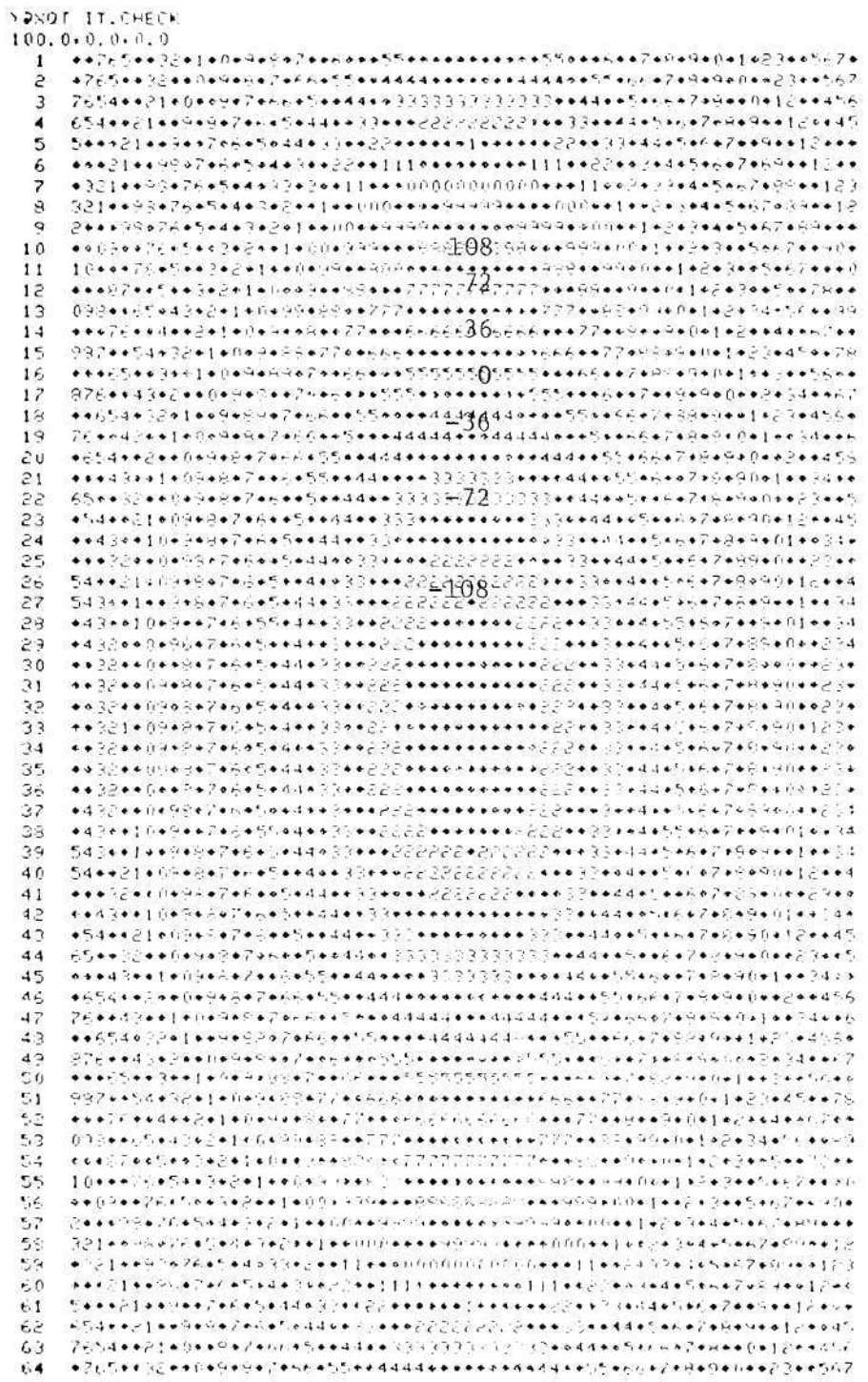

Figure 7. A Computer Generated Phase Map of a Uniform Phase and Amplitude Plane Wave Spectrum that Has Been Shifted to a New Location in Space, i.e., x = 100, y = 0, z = 0 cm. This Phase map Represents the Phase Variation Over a ±20° Angular Sector. (The Scale of 0 to 10 Corresponds to a Range of -180° to +180°.)

the stationary phase point shifts away from the center to the fourth quadrant as shown in Figure 8, and again a relatively rapid phase variation with k_y and k_z away from the stationary phase point occurs.

For a uniform circular aperture, the number of lobes in the integrand is approximately an arc-sine relationship with respect to radial wavenumbers [19,21] as given by

$$N_{lobes} = \frac{\sin^{-1} k_\rho}{\pi} \left(\frac{a}{\lambda} + \frac{\rho}{\lambda} + \frac{x}{\lambda}\right) \tag{17}$$

where $k_\rho = \sqrt{k_y^2 + k_z^2}$ is the normalized radial wavenumber,

x is the field point distance in wavelengths from the aperture plane,

a is the semi-largest dimension of the aperture (radius, if circular), and

ρ is the transverse field point component on the aperture plane.

The integration time required to compute the near field corresponds directly to the number of lobes used in the computation. However, the arc-sine relation of Equation (17) exists between the number of lobes in the integrand and the radial wavenumber. Because of this relationship, the required integration time for a 0.707 x 0.707 wavenumber region, rather than one 0.5 x 0.5, would be only one half the integration time required to integrate over the entire visible wavenumber circle. The number of lobes in transverse wavenumber directions for the aperture is also approximately an arc-sine relationship, but this relation is also dependent upon radial wavenumbers. Thus, an integrand requiring α lobes at a radial wavenumber of $K_\rho = 0.707$ would require α

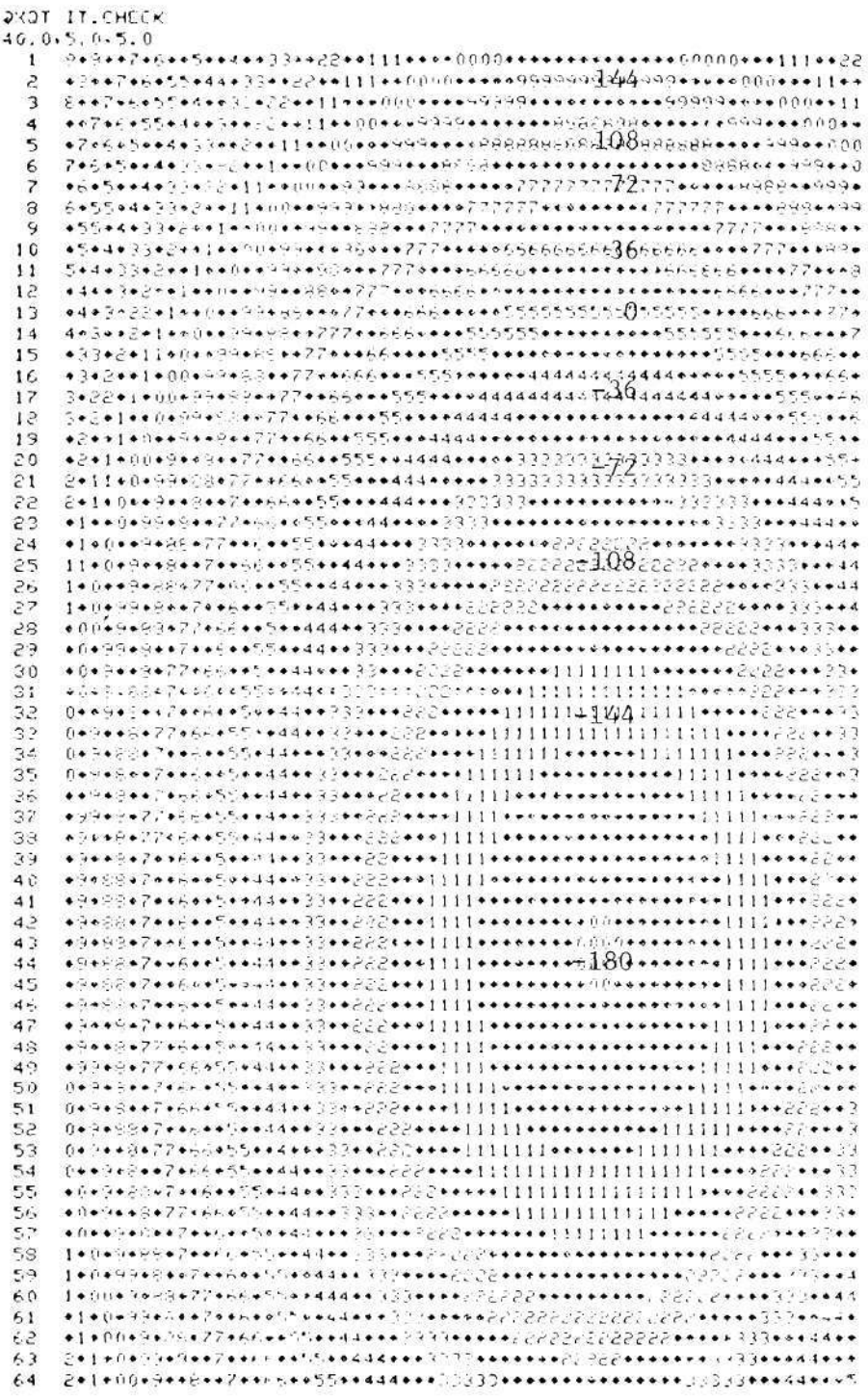

Figure 8. A Computer Generated Phase Map of a Uniform Phase and Amplitude Plane Wave Spectrum that Has Been Shifted to a New Location in Space, i.e., x = 40, y = 5, z = 5 cm. This Phase Map Represents the Phase Variation Over a $\pm 20°$ Angular Sector. (The Scale of 0 to 10 Corresponds to a Range of -180° to +180°.)

(1.0/0.707) lobes in the transverse wavenumber direction, as given by

$$N_{lobes} = \alpha \frac{\sin^{-1}(k_\rho)}{\sin^{-1}(K_\rho)} \quad . \tag{18}$$

However, as the radial wavenumber distance increases, Equation (18) indicates that the required number of lobes in the integrand for transverse wavenumbers would become less than α. This is illustrated by the behavior of the size of the stationary phase region shown in Figures 6 and 7. Thus, for close-in near-field distances it is obvious that a greater number of transverse wavenumber samples are required than for farther-out near-field distances.

The integration technique known as the Saddle Point integration or the Method of Steepest Descents [22,23] permits an analytical expression to be derived for the near-field integral of Equation (14) if the functional form of the spectrum is known. However, this is not the case for measured antenna data, and it is thus important to determine the minimum number of spectral samples which are required to numerically determine the integral.

Consider that the near field on the plane $x = d_1$ in Figure 9 is known either by measurement or by calculation using the known and complete visible wavenumber spectrum. It is then possible to compute the near field over an angular sector of interest at a distance $x = d_2$ from the antenna using numerical quadrature techniques to evaluate the integral of Equation (14). The purpose of this investigation is to determine an efficient computational method which will allow accurate

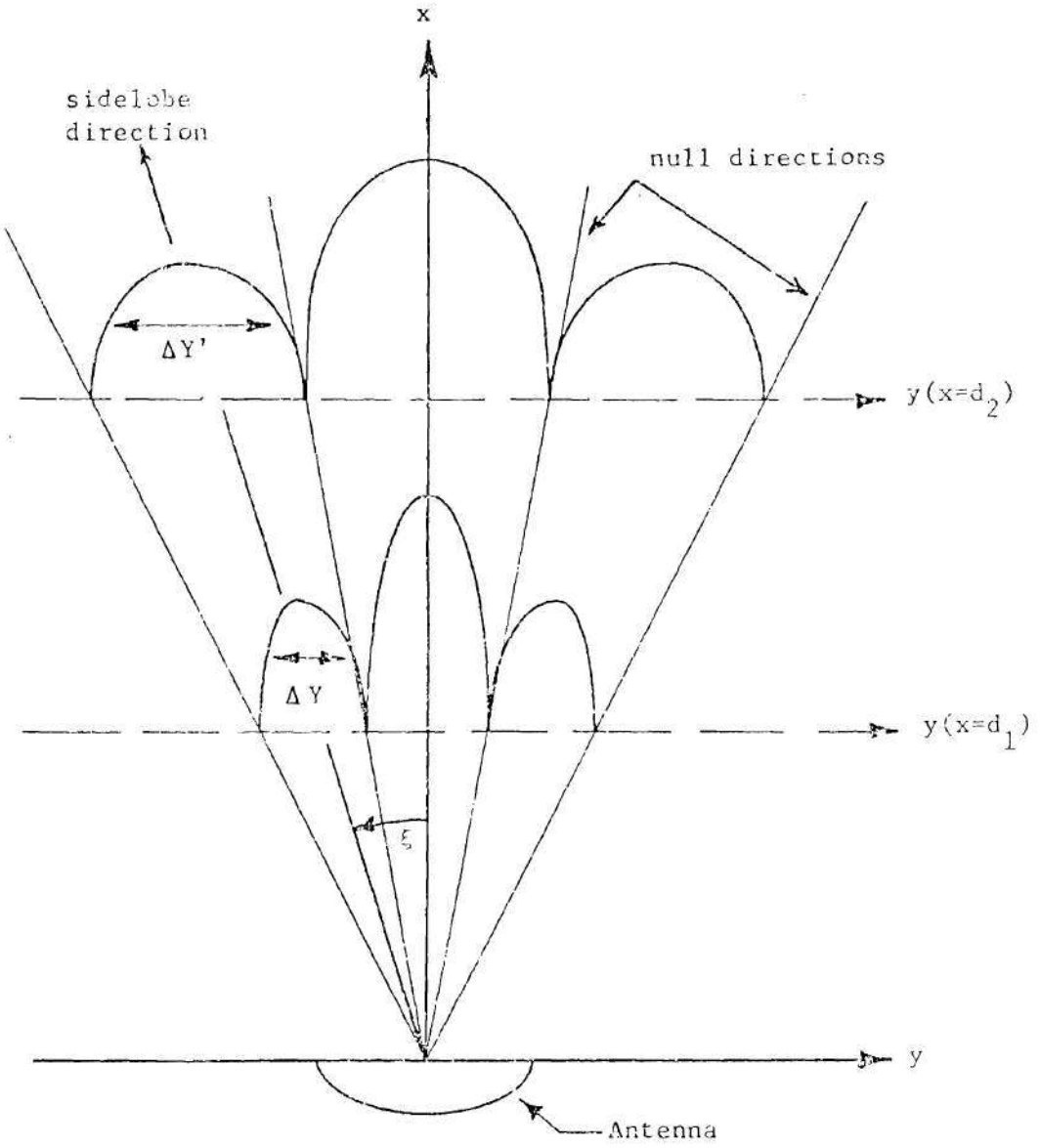

Figure 9. An Illustration of the Near-field Radiation Pattern on Two Different Near-field Planes Located at $x=d_1$ and $x=d_2$.

computation of the near field on a specified sector of the plane located at $x = d_2$ without using the entire visible wavenumber spectrum.

A quasi-optical technique for determining the number of spectral samples required to accurately describe the near-field of an antenna in a particular region will now be presented. The angular near-field sector of interest (as viewed from the source) is used to determine, to a first order approximation, the size of the spectral region needed to describe the field. The procedure involves (1) determining the near-field angular sector of interest, (2) mapping this region into wavenumber space, (3) determining the location and extent of this wavenumber region, and (4) employing the size of the wavenumber region and the wavenumber sample spacing to determine the required number of spectral samples.

The approach presented here is to limit the number of spectral samples to the region of spectrum space which makes the dominant contribution to the field in a specified spatial sector. For the angular sector shown in Figure 10(a) lower and upper wavenumber bounds on the angular sector of interest are chosen to be

$$\begin{aligned} k_{yLB} &= k_o \sin \theta_{LB} \sin \phi_{LB} \\ k_{yUB} &= k_o \sin \theta_{UB} \sin \phi_{UB} \end{aligned} \tag{19}$$

and

$$\begin{aligned} k_{zLB} &= k_o \cos \theta_{LB} \\ k_{zUB} &= k_o \cos \theta_{UB} \end{aligned} \tag{20}$$

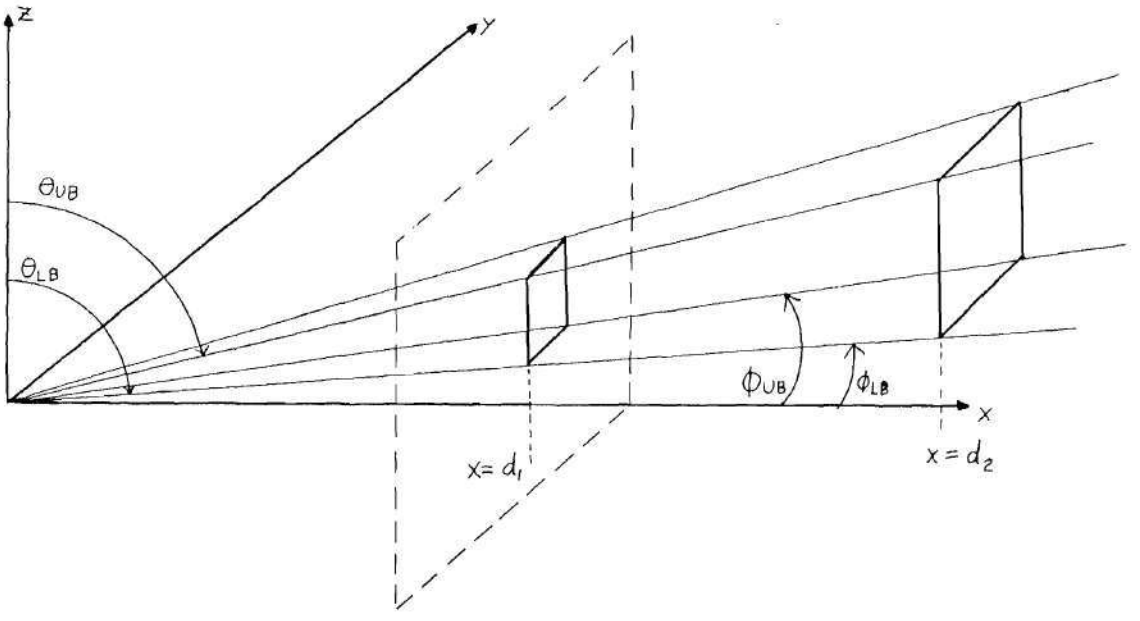

(a) Angular sector located in (θ,ϕ) space.

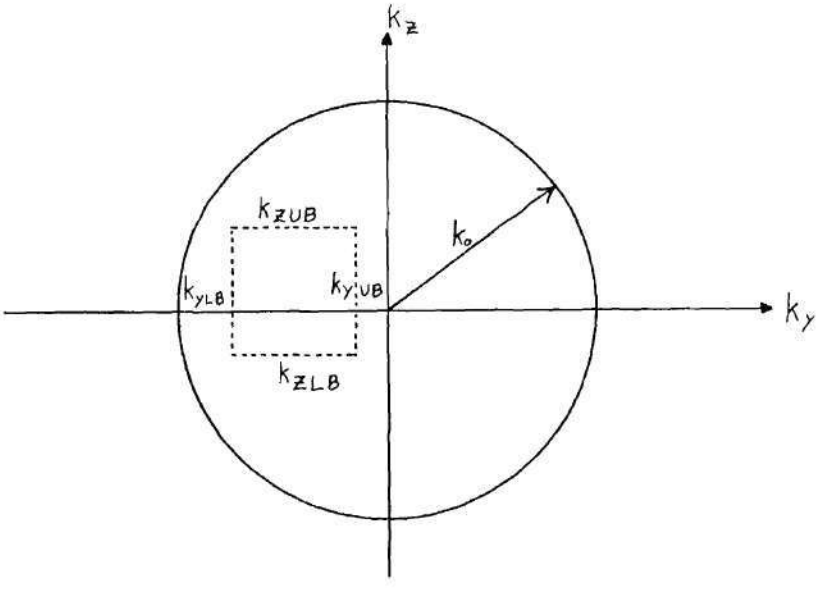

(b) Quasi-optical projection of sector into wavenumber space.

Figure 10. Mapping of Angular Sector of Near Field into Wavenumber Space.

where LB and UB represent the lower and upper regional bounds, respectively, and only angles in the forward hemisphere are considered. This bounded wavenumber region is shown in Figure 10(b). Equations (19) and (20) represent a mapping of the (θ,ϕ) sector of Figure 10(a) into wavenumber space by an "optical projection." This projection results in using a wavenumber limited version of the spectrum to compute the fields over the specified angular sector. Thus, in this method, the visible wavenumber limits $\pm\sqrt{k_y^2 + k_z^2} \leq k_o$ of integration on the integrals of Equation (14) are effectively replaced by the wavenumber limits determined from Equations (19) and (20). This quasi-optical technique for determining the size and location of the wavenumber region has been employed in numerical computations to determine the number of spectral samples required to compute the near field of an antenna over a limited near-field sector. Results of the numerical study are presented in Chapter IV, and these results indicate that this method is accurate, efficient, and useful in near-field computation.

The optical projection approach is related to the quasi-optical propagation of Gaussian beams. In fact, the optical paths predicted by Equations (19) and (20) are the straight-line asymptotes to the hyperbolic phase paths of a Gaussian beam, which is a special case of a ray-optical field that can be represented in terms of local plane waves. A ray optical field of the form

$$\bar{E}(r) = \bar{A}(r)\, e^{-jkS(r)} \tag{21}$$

represents a wave which is locally plane and can be used to obtain an asymptotic solution to the Sommerfeld-Runge ray optics form of the wave

equation [25]. The substitution of Equation (21) into the Helmholtz equation yields

$$(\nabla^2 + n^2 k_o^2)\, \bar{E}(r) = 0 \tag{22}$$

where n is a function of the position vector $\bar{r}$ results in the equation

$$k_o^2(n^2 - (\nabla S)^2) + ik_o(\nabla^2 S + 2\nabla S \cdot \frac{\nabla A}{A} + \frac{\nabla A}{A}) = 0 \tag{23}$$

where A represents the amplitude of the vector field $\bar{A}$. This result is composed of three terms which are written here in decreasing order of magnitude with respect to k_o. If the third term is neglected, Equation (23) is satisfied when the first two terms are zero. The first term is the eikonal equation

$$(\nabla S)^2 = n^2 \ . \tag{24}$$

The second term of the equation

$$\nabla^2 S + 2\nabla S \cdot \frac{\nabla A}{A} = 0 \tag{25}$$

can be shown [26] to represent the transport properties of the field intensity. In order for the quasi-optics approximation to be valid, the *third term* $\frac{\nabla A}{A}$ *must be zero. This is not the* case near a focus or on a caustic surface where, as a result of neglecting this term, ray optics predicts an infinite field.

The Luneberg-Kline derivation of ray optics proceeds directly from Maxwell's equations by using an expansion of the electromagnetic field in inverse wavenumbers [27]. In the Luneberg-Kline derivation, the scalar

amplitude A of the Sommerfeld-Runge form is replaced by the vectors $\overline{E}$ and $\overline{H}$. It was found that S satisfies the same eikonal equation as in the scalar case and therefore, the rays can be constructed in the same manner where the transport equations indicate the variation of $\overline{E}$ and $\overline{H}$ along each ray [27]. The result is that the relations between $\overline{E}$, $\overline{H}$, $\overline{k}$ are the same as in a plane wave.

A Gaussian beam field which satisfies ray-optics and the paraxial wave equation resulting from the optical derivation can be constructed from given initial conditions. The plane x = 0 is an equiphase plane on which the field is given by

$$\overline{E}_{x=0} = \overline{A}\, e^{-kI} \tag{26}$$

and

$$S = R - jI, \tag{27}$$

where R and I are orthogonal components of the complex phase S. Then to determine the field for x > 0, we seek a solution

$$y = y(x,q) \tag{28}$$

for a typical phase path that leaves the x = 0 plane at y = q, where q is a path-distinguishing parameter. For a pencil of rays which are normal to the wavefront, the solution for this phase path is given by Choudhary and Felsen [28] as

$$y(x,q) = q(1 + Mx^2)^{1/2} \tag{29}$$

where $M = 4/n^2w^2$ and w is the beam waist.

Choudhary and Felsen [28] demonstrate that Equation (29) must represent a hyperbolic phase path for Gaussian beam propagation. Thus, the projection directions in the far zone are the straight-line asymptotes of the hyperbolic Gaussian ray paths. Because of this fact, we note that the optical projection method previously described uses the far-zone asymptotes specified by Equations (19) and (20) to determine the approximate wavenumber space which corresponds to a particular region of the near field where the ray propagation is hyperbolic. However, we will see that this is a good approximation at intermediate near-field ranges.

The propagation of Gaussian beams is also related to the uncertainty principle. Thus, if the size of the regions used to compute the near field over a given angular sector is to be necessary and sufficient, it satisfies the uncertainty principle. For the case of a Gaussian wave packet or equivalently, a Gaussian signal (from Fourier Transform Theory), the minimum uncertainty condition is met and the asymptotic limit of the Gaussian phase paths predicted by the quasi-optics technique will be shown to be valid in the following paragraphs. If the wave is not Gaussian, minimum uncertainty is not met and a larger wavenumber region must be used to accurately describe the near field in a given sector.

Consider the propagation of waves in a homogeneous, isotropic medium. The simplest type is a plane monochromatic wave of the form

$$\Psi_1 = e^{j(\omega t - \bar{k} \cdot \bar{r})} \tag{30}$$

propagating in the direction of the wavenumber vector $\bar{k}$ with constant velocity and wavelength $2\pi/k$. The propagation velocity is the velocity

of propagation of planes of equal phase; that is, the phase velocity,

$$v_\phi = \frac{\omega}{k} . \tag{31}$$

Ths function Ψ, given by Equation (30) does not enable the distinction between different points in space and time; therefore, the intensity of the wave motion is the same everywhere. However, the general wave field obtained by adding several wave functions of this form can be described by

$$\overline{\Psi} = \int_{-\infty}^{\infty} \int_{-\infty}^{\infty} \overline{A}_s(\overline{k})\ e^{j(\omega t - \overline{k} \cdot \overline{r})} dk_y dk_z \tag{32}$$

which is a two-dimensional wave packet of finite extension, where $\overline{A}_s(k)$ is a special spectral wave function also of limited extension. This procedure corresponds to applying the superposition principle to deBroglie waves where each frequency ω is associated with a well defined energy of a particle. DeBroglie waves travel with the velocity

$$v_g = \frac{d\omega}{dk} \tag{33}$$

which is the group velocity of the wave $e^{j(\omega t - \overline{k} \cdot \overline{r})}$. For the case of a homogeneous medium, v_g is equal to the phase velocity v_ϕ given by Equation (31). Kramers [29] states "the fact that one can choose at a given time the value of the wave function obtained by superposition of plane waves indicates how one should connect the concept of matter waves with the classical idea of localization in space and time of a particle." From this and Equations (31) and (32), we see that the group velocity

of matter waves is equal to the velocity of the mass point in classical theory [30].

In Equation (32), $\bar{A}_s(k)$ is the complex amplitude function. If $\bar{\Psi} = \bar{\Psi}_o$ at $t = 0$, $\bar{A}_s(k)$ will be uniquely determined as

$$\bar{A}_s(\bar{k}) = \int_{-\infty}^{\infty} \int_{-\infty}^{\infty} \Psi_o \, e^{j\bar{k}\cdot\bar{r}} dydz \tag{34}$$

A special wave packet is characterized by the fact that $|\bar{\Psi}_o|$ is of significant value only in the neighborhood of y_o, z_o while the same holds for $|\bar{A}_s|$ only in the neighborhood of k_{y_o}, k_{z_o}. If the phase of $\bar{\Psi}_o$ changes very little over a region U near y_o, z_o, from Equation (34) we obtain

$$\bar{A}_s(k_y,k_z) = \int_{-\infty}^{\infty} \int_{-\infty}^{\infty} \Psi_o \, e^{j[(k_y-k_{y_o})y+(k_z-k_{z_o})z]} dydz. \tag{35}$$

If $k_y - k_{y_o}$ becomes large enough that $(k_y - k_{y_o})y$ can vary by a few units within U, $|\bar{A}_s|$ will be negligible compared to its value for $k_y = k_{y_o}$, $k_z = k_{z_o}$. If Δy is denoted as the approximate extension of U in the y-direction and Δk_y is denoted as the range of k_y values for which $|\bar{A}_s|$ is appreciably different from zero, we obtain the relation [29,30]

$$\Delta y \, \Delta k_y \simeq 1 \tag{36}$$

If Δy, Δk_y are properly defined, it is possible to exactly determine the minimum value of the product $\Delta y \, \Delta k_y$. Multiplying $\bar{\Psi}_o$ by a constant chosen such that

$$\int_{-\infty}^{\infty} \int_{-\infty}^{\infty} |\bar{\Psi}_o|^2 \, dydz = 1 \, , \tag{37}$$

y_o may be defined as

$$y_o = \int_{-\infty}^{\infty} \int_{-\infty}^{\infty} |\bar{\Psi}_o|^2 \, dydz \tag{38}$$

and Δy as

$$(\Delta y)^2 = \overline{(y - y_o)^2} = \int_{-\infty}^{\infty} \int_{-\infty}^{\infty} \overline{(y-y_o)^2} \, |\bar{\Psi}_o|^2 dydz \tag{39}$$

The quantity y_o measures the position of the wave and Δy, its extension. From Equations (34) and (37) it follows that

$$\int_{-\infty}^{\infty} \int_{-\infty}^{\infty} |\bar{A}_s|^2 \, dk_y dk_z = 1 . \tag{40}$$

Now k_{y_o} is defined as

$$k_{y_o} = \int_{-\infty}^{\infty} \int_{-\infty}^{\infty} k_y |\bar{A}_s|^2 \, dk_y dk_z \tag{41}$$

and Δk_y as

$$(\Delta k_y)^2 = \overline{(k_y - k_{y_o})^2} = \int_{-\infty}^{\infty} \int_{-\infty}^{\infty} (k_y - k_{y_o})^2 |\bar{A}_s|^2 dk_y dk_z \tag{42}$$

The quantity k_{y_o} measures the average wavenumber represented in the wave packet and Δk_y, its extension in wavenumber space. The equations for the z-component are analogous. The minimum value which $\Delta y \, \Delta k_y$ can attain is given by the equation [29]

$$(\Delta y \, \Delta k_y) = \frac{1}{4\pi} . \tag{43}$$

This minimum is attained if these wave packets correspond to Gaussian distributions for both $|\overline{\Psi}_o|^2$ and $|\overline{A}_s|^2$. Similar conditions also hold in Fourier Transform Theory for the case of a signal f(t) and its Fourier transform $F(\omega)$ [31]. If $|f(t)|^2$ and $|F(\omega)|^2$ correspond to Gaussian distributions, the minimum uncertainty condition holds. This result will be seen to correlate with the size of the region projected using the quasi-optics asymptotic projection for Gaussian beams in Chapter IV. If the field distribution is not Gaussian, but say parabolic, the minimum uncertainty condition no longer holds and the projected $\Delta y\ \Delta k_y$ will be greater than for minimum uncertainty. Therefore, a spatial sector of extension Δy will require the wavenumber region of extent Δk_y to be larger than that required for a Gaussian field distribution.

The question as to the sufficient uncertainty for a given wave spectrum can be addressed by having a complete knowledge of the field on a plane located at $x = d_1$ (Figure 9). This field can be measured or computed using the entire known visible spectrum. The quasi-optics approach is then employed to compute the field over the angular sector of interest at the $x = d_1$ plane. Comparing these results over the given angular sector checks the convergence of the near field computed from the bandpass filtered spectrum. Once convergence is obtained for a given sector, the corresponding wavenumber region may be used to efficiently compute the near field over that sector for any farther-out near-field distance.

Now let us relate the above quasi-optical, Gaussian beam, and stationary phase properties to the complete plane wave spectrum function

via an example. Figure 11 illustrates a spectrum which exhibits distinct lobes and possesses the ideal far-field property of a 180° phase inversion between lobes. As we have seen from the computed phase maps shown in Figures 6 and 7, the stationary phase region becomes smaller as one moves further out along the x-axis. The phase oscillations of the integrand of Equation (15) become more and more rapid as the distance increases, as illustrated in Figures 7 and 11. Expressing the spectrum of Figure 11 as a linear combination of spectral contributions,

$$\bar{A} = \sum_{i=1}^{n} \bar{A}_i \tag{44}$$

where $\bar{A}_i = \bar{A}$ on the i^{th} interval and zero elsewhere.

The electric field is related by a Fourier transform as

$$\bar{E} = \frac{1}{2\pi} \int_{-k_{zm}}^{+k_{zm}} \int_{-k_{ym}}^{+k_{ym}} \bar{A}\, e^{-j(k_y y + k_z z)}\, dk_y dk_z, \tag{45}$$

or equivalently,

$$\bar{E} = \frac{1}{2\pi} \int\int \sum_{i=1}^{n} \bar{A}_i\, e^{-j(k_y y + k_z z)}\, dk_y dk_z \; . \tag{46}$$

As seen from the phase map of Figure 8, a stationary phase region in the angular direction of a lobe such as that included in the quasi-optics region of Figure 11 also exists. Because the integral is uniformly convergent, the order of the sum and the integral may be interchanged and we write

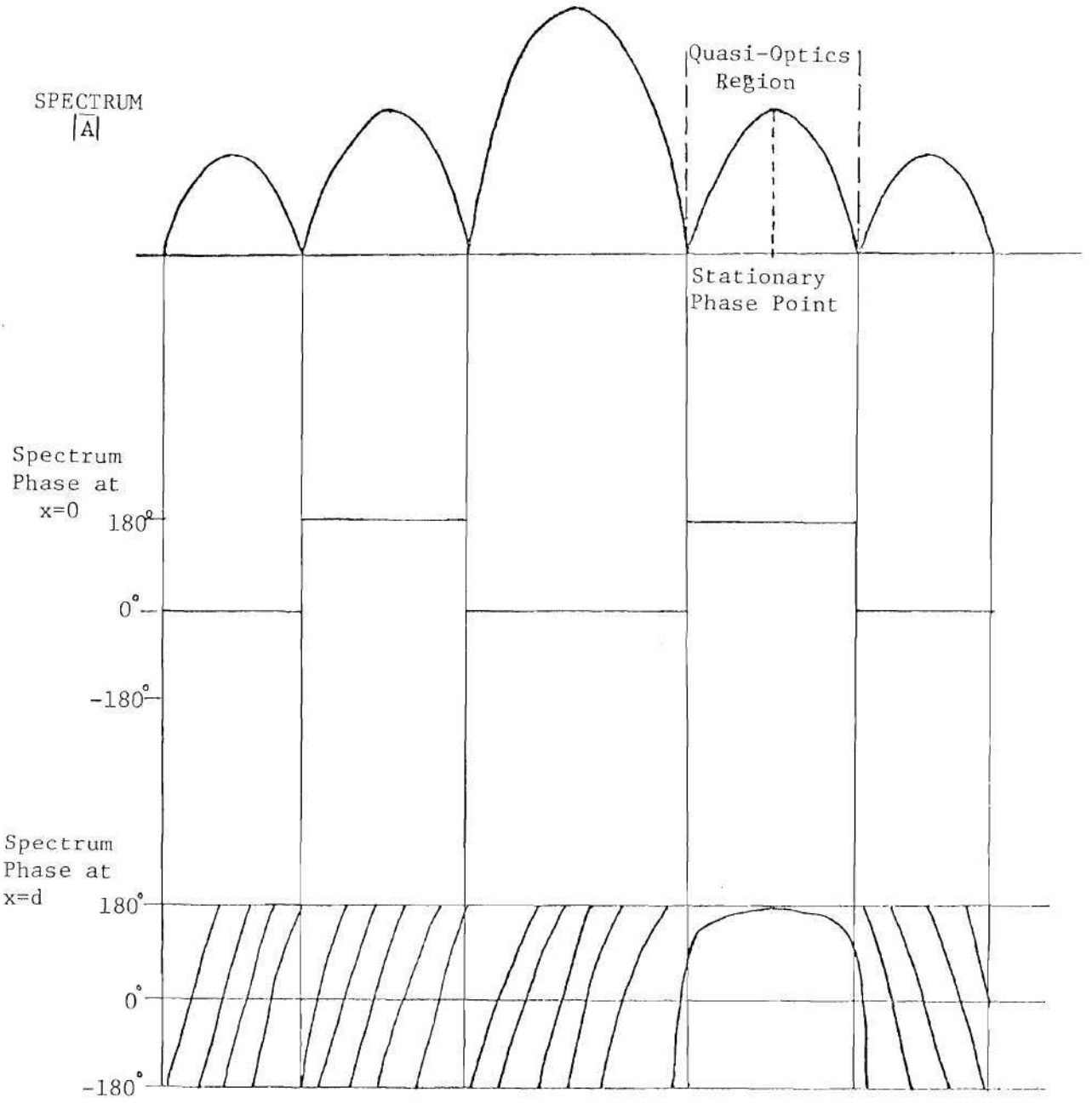

Figure 11. Example of Spectrum Function Showing Stationary Phase Region at x=d Plane

$$\bar{E} = \frac{1}{2\pi} \sum_{i=1}^{n} \int\int \bar{A}_i \, e^{-j(k_y y + k_z z)} \, dk_y dk_z \tag{47}$$

and

$$\bar{E} = \frac{1}{2\pi} \left[\int\int_{\substack{i=\text{stationary} \\ \text{phase region}}} A_s e^{-j(k_y y + k_z z)} + \sum_{\substack{i=1 \\ i \neq s}}^{n} \int\int \bar{A}_i e^{-j(k_y y + k_z z)} \right] dk_y dk_z \tag{48}$$

where

$$\sum_{\substack{i=1 \\ i \neq s}}^{n} \int\int \bar{A}_i e^{-j(k_y y + k_z z)} \longrightarrow 0$$

by the principle of stationary phase. Therefore, $\bar{A}_s$ is a "special wave packet" corresponding to the stationary phase region. The entire spectrum may be used to evaluate the integral, but it is not required since the regions outside the stationary phase region do not contribute to the result. Therefore, the wavenumber limits may be reduced to include only the region, described by the quasi-optics, which contains the significant field contributions.

The results of this study, which are presented in Chapter IV, have shown that the quasi-optics technique for predicting the size and location of the wavenumber bandpass filtered region yields accurate results at near-field distances as close in as $0.05D^2/\lambda$. At this distance, for aperture antennas, the lobe structure of the near-field pattern is reasonably well defined. This correlates with experimental results [32] which have indicated that the angular locations of the nulls in the

measured polar near-field pattern of a 13λ circular phased array are defined at a distance of less than $0.03D^2/\lambda$. Figure 12 indicates the phase error $\Delta\phi$ which results from the error r' due to using a planar surface as an approximation to a spherical wavefront. The distance d represents the distance from the antenna to the near-field computation plane which is given by

$$d = \frac{r'}{1 - \cos \Delta\theta} . \tag{49}$$

The relative phase error $\Delta\phi$ is given by

$$\Delta\phi = \frac{2\pi}{\lambda} (r') \tag{50}$$

where

$$r' = d(1 - \cos \Delta\theta) . \tag{51}$$

For d to be in the near field of an antenna, the distance r' (which represents the phase error) must be greater than 0.0625λ which corresponds to the far-field distance $2D^2/\lambda$. For the case of an 8λ aperture where accurate results were obtained at $d = 0.05D^2/\lambda$, r' = 1.09λ which results in a relative phase error indicative of being well into the near-field region. Obviously, the quasi-optics projection could be extended into the far field since the ray paths of this optical projection represent the far-field straight-line asymptotes of hyperbolic Gaussian phase paths. However, as the distance from the antenna is increased, other computational techniques such as the aperture field method become competitive in terms of computation time. A comparison of computation times for the aperture field method and the PWS technique are presented in Chapter IV.

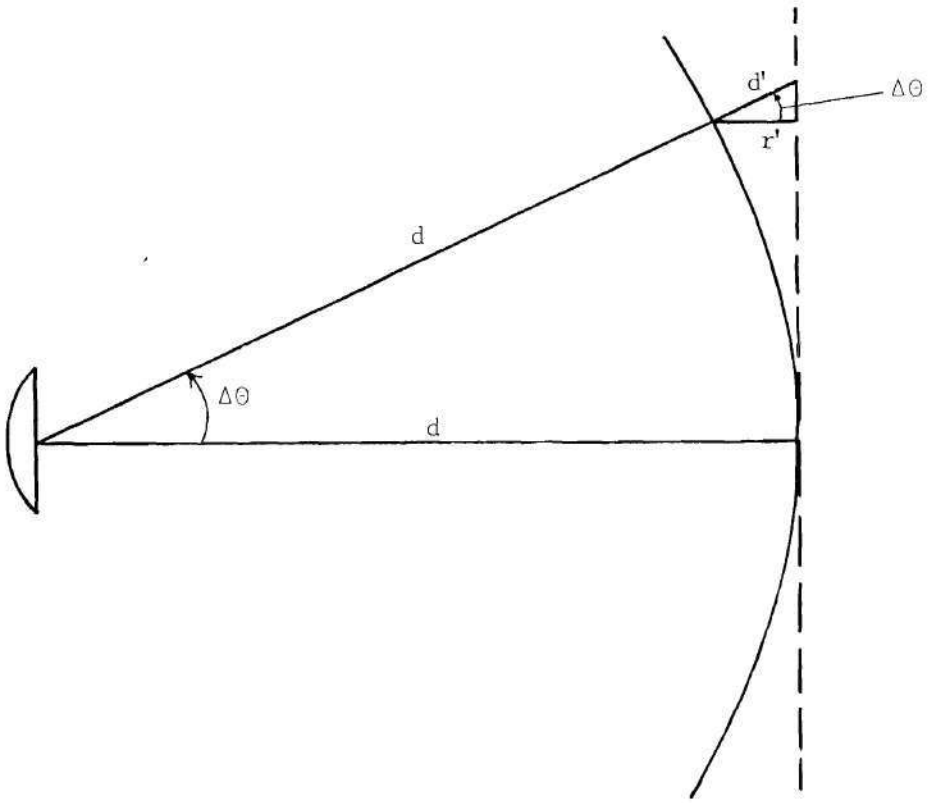

Figure 12. Diagram Showing the Relative Error r' Resulting from Using a Planar Approximation for a Spherical Wavefront.

CHAPTER III

NUMERICAL CONSIDERATIONS

Limitation on Near-Field FFT Computations

The antenna far field, which is proportional to the antenna plane wave spectrum, can be efficiently computed using the discrete Fast Fourier Transformation (FFT) algorithm. However, the direct application of the FFT algorithm to the determination of the near fields from the PWS integral encounters computational problems if a large sector of the near field is to be determined. The following derivation demonstrates a fundamental limitation on discrete FFT processing to determine the near fields and discusses techniques for overcoming this limitation.

In order for the FFT algorithm to be accurate in determining the spectrum $\overline{A}$ over a "full" forward hemisphere (2π steradians), it is necessary that the aperture distribution be sampled at intervals $\delta \leq \lambda/2$, that is, at the Nyquist sample rate. The maximum wavenumber along the y-axis of the aperture plane $k_{y(max)}$ is related to the sample spacing δy by

$$k_{y(max)} = \pi/\delta y \ . \tag{52}$$

When $\delta = \lambda/2$, the maximum wavenumber $k_{max} = k_o = \frac{2\pi}{\lambda}$, and the antenna fields can be determined over the full forward hemisphere. If an $N \times N$ sample space is used corresponding to the visible wavenumber region $-k_{ymax} < k < +k_{ymax}$, the wavenumber sample spacing δk_y is

$$\delta k_y = \frac{2k_{y(max)}}{N} \tag{53}$$

The maximum linear distance y_m from the antenna center ($y = 0$, $z = 0$) at which the fields are sampled is simply the number of samples taken for $y < 0$ times the spatial sample spacing, i.e., $y_m = \frac{N}{2}\,\delta y$. Thus, the wavenumber spacing δk_y is related to the linear distance y_m by

$$\delta k_y = \pi / y_m \ . \tag{54}$$

One can demonstrate that a measurement taken at a spacing of δy over a maximum dimension of $-y_m \leq y \leq y_m$ on the y-z measurement plane located at $x = d_1$ as shown in Figure 13 is not sufficient to determine the field over the complete angular sector shown in Figure 13 on a plane located at $x = d_2$. On the plane located at $x = d_2$, the maximum y-dimension within the linear sector designated y_m' is greater than the maximum distance y_m over which the fields were originally sampled on the plane $x = d_1$. However, from Equation (54), the wavenumber spacing $\delta k_y'$ which is required for an accurate representation of the fields over the planar surface at $x = d_2$ is given by

$$\delta k_y' = \ /y_m' \ , \tag{55}$$

which implies that $\delta k_y' < \delta k_y$ because $y_m' > y_m$. That is, smaller wavenumber spacing must be used to determine the fields over the plane at $x = d_2$. However, for cases where measured data exists only on the $x = d_1$ plane, we have $\delta k_y' = \delta k_y$ rather than $\delta k_y' < k_y$ as required for determining the near field over the entire $x = d_2$ plane. Therefore, the field over the $x = d_2$ plane can be predicted only over an area equal to the

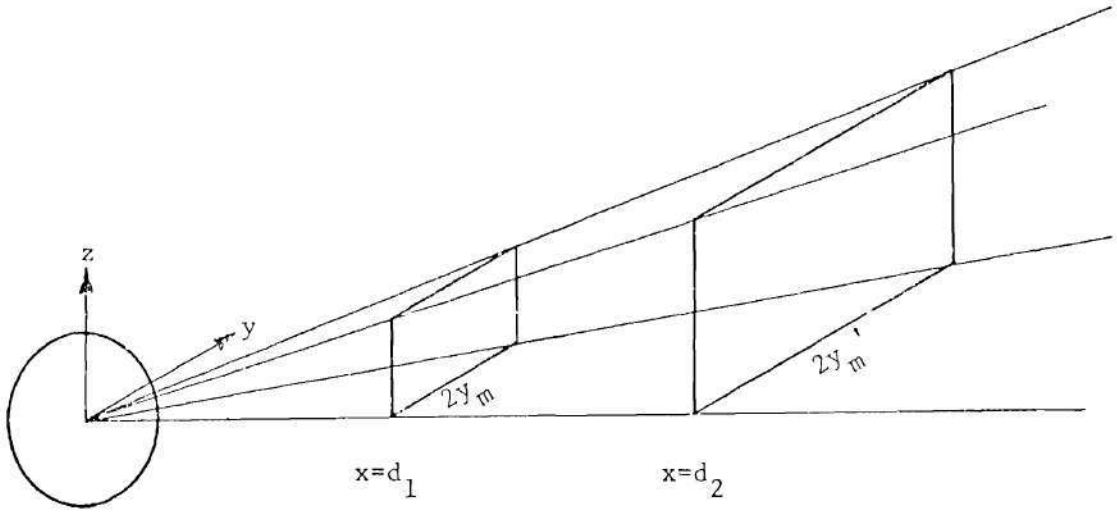

Figure 13. Diagram of the Relation Between the Near-field Planes Located at Ranges of $x=d_1$ and $x=d_2$ and the Angular Region Subtended by their Boundaries.

original measurement unless a smaller wavenumber sample spacing is employed, resulting in a corresponding increase in the number of near-field samples which must be processed.

This is illustrated in Figure 14 where $k_{y(max)}' = k_{y(max)}$ which restricts calculation of the near field over the $x = d_2$ plane to a region no larger than that of the measurement plane. The near field over the entire $x = d_2$ plane can be determined only if a sufficient number of samples are included in the original measured data to ensure a wavenumber sample rate such that $\delta k_y' < \delta k_y$. Similar relationships hold for sample points located along the z-axis of the measurement plane. In that case,

$$\delta k_z = \pi / z_m \ , \tag{56}$$

and

$$\delta k_z' = \pi / z_m' \ , \tag{57}$$

which implies that $\delta k_z' < \delta k_z$ because $z_m' > z_m$. However, $k_{z(max)}' = k_{z(max)}$ and once again calculation of the near field is restricted to an equivalent size plane at $x = d_2$ unless the wavenumber sample spacing is decreased by increasing the number of near-field samples.

However, the problems associated with the discrete FFT can be avoided by computing the near field using direct numerical quadrature. An integration technique which interpolates between the sampled data points is attractive for this application and one such technique is a Bivariate integration rule [33]. This quadrature rule employs a linear

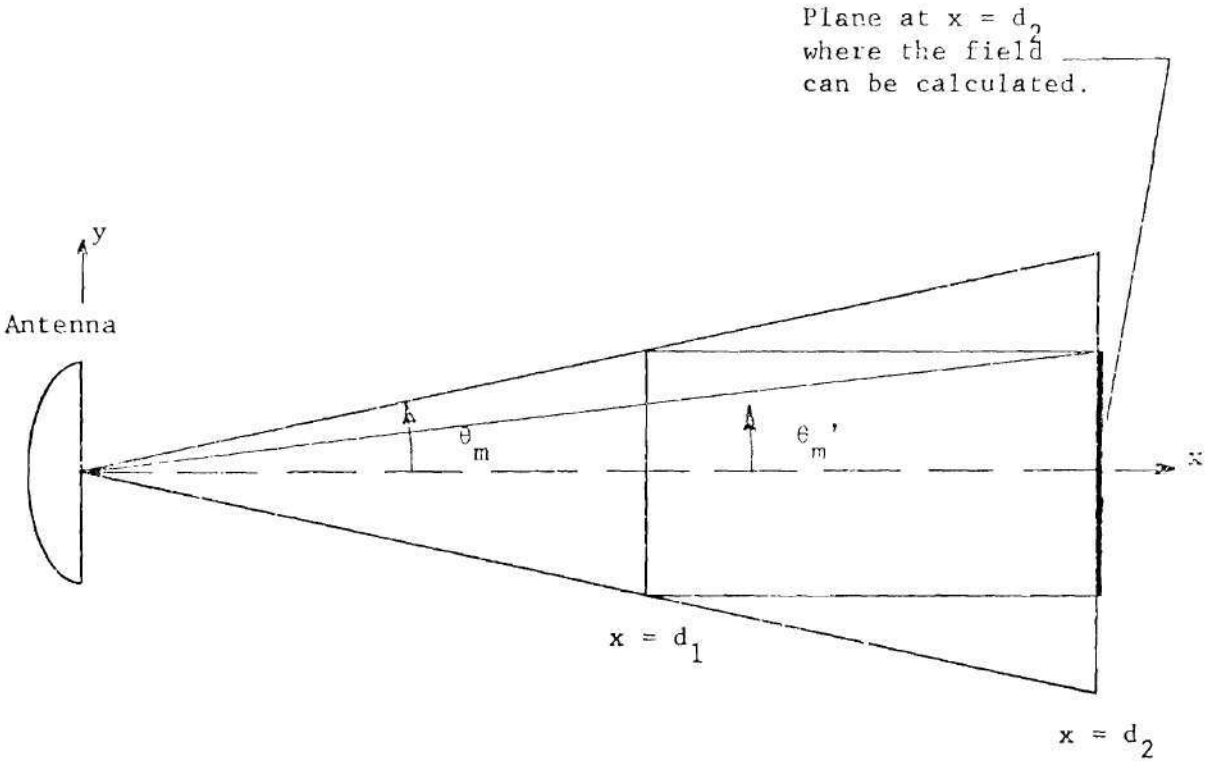

Figure 14. Two Dimensional View of the Near-field Planes Located at $x=d_1$ and $x=d_2$ with the Corresponding Angular Region Subtended by their Boundaries.

interpolation to approximate the value of the integrand in the intervals between the sampled data points. For an integrand which is a function of two variables, such as the spectrum function $\bar{A}(k_y,k_z)$ which is used to compute the near field, the Bivariate integration rule approximates the function using a four-point linear interpolation [34]. The integration rule which was used in this study to compute the antenna near-zone fields computes the values of the integrals of Equation (15), restated here as

$$\bar{E}(x,y,z) = \frac{1}{2\pi} \int_{-k_{z(max)}}^{k_{z(max)}} \int_{-k_{y(max)}}^{k_{y(max)}} \bar{F}(k_y,k_z,x) e^{-j[k_y y + k_z z]} dk_y dk_z . \tag{15}$$

The details of the Bivariate quadrature rule are summarized in the Appendix. When this quadrature rule is employed, the sample spacing must be chosen such that any rapid phase variations of the function $\bar{F}(k_y,k_z,x)$ due to the x-dependent phase term Δk_y and Δk_z are adequately sampled. Other quadrature rules such as the Newton-Cotes or Gauss formulas can also be used [34].

However, the Newton-Cotes or Gauss integration formulas approximate the entire integrand, whereas the Bivariate quadrature rule approximates only the function $\bar{F}(k_y,k_z,x)$ using a linear interpolation. This technique, which is similar to the Filon quadrature rule [34], results in a more efficient computer evaluation of integrals of the type given by Equation (15).

Computational Process

The concept of wavenumber bandpass filtering which was developed

in the preceding chapter was implemented in a computer algorithm to investigate its practical application to the computation of near-zone antenna fields. The algorithm for the numerical solution of Equation (14) was written such that discrete points could be employed to describe the illumination function over the x = 0 plane. This permits the accuracy of the solution for illumination functions treated as discrete measured data points, which is a common method of near-field pattern measurements, to be examined. These discrete samples were used to compute the near-zone patterns of uniformly illuminated 8λ and 16λ square apertures.

The calculation of the near-zone radiation patterns of the sampled aperture illumination function was performed on Georgia Tech's UNIVAC 1108 and CYBER 74 digital computers. The computation process is shown in the block diagram of Figure 15. The input for the computation process consists of a theoretical illumination function which is sampled every $\lambda/2$ and the resulting amplitude and phase information stored in a 64 by 64 complex array. In this same manner, the measured near field of a particular test antenna could also be stored in the data array. However, the spectra of the measurement probe would have to be determined and incorporated into the algorithm to correct the wavenumber spectrum of the measured test antenna. Each point in this complex data array represents the amplitude and phase of the y-component in the near field, sampled every one-half wavelength in the y and z directions.

The plane wave spectrum of the sampled illumination function is computed using a two-dimensional discrete FFT. This plane wave spectrum

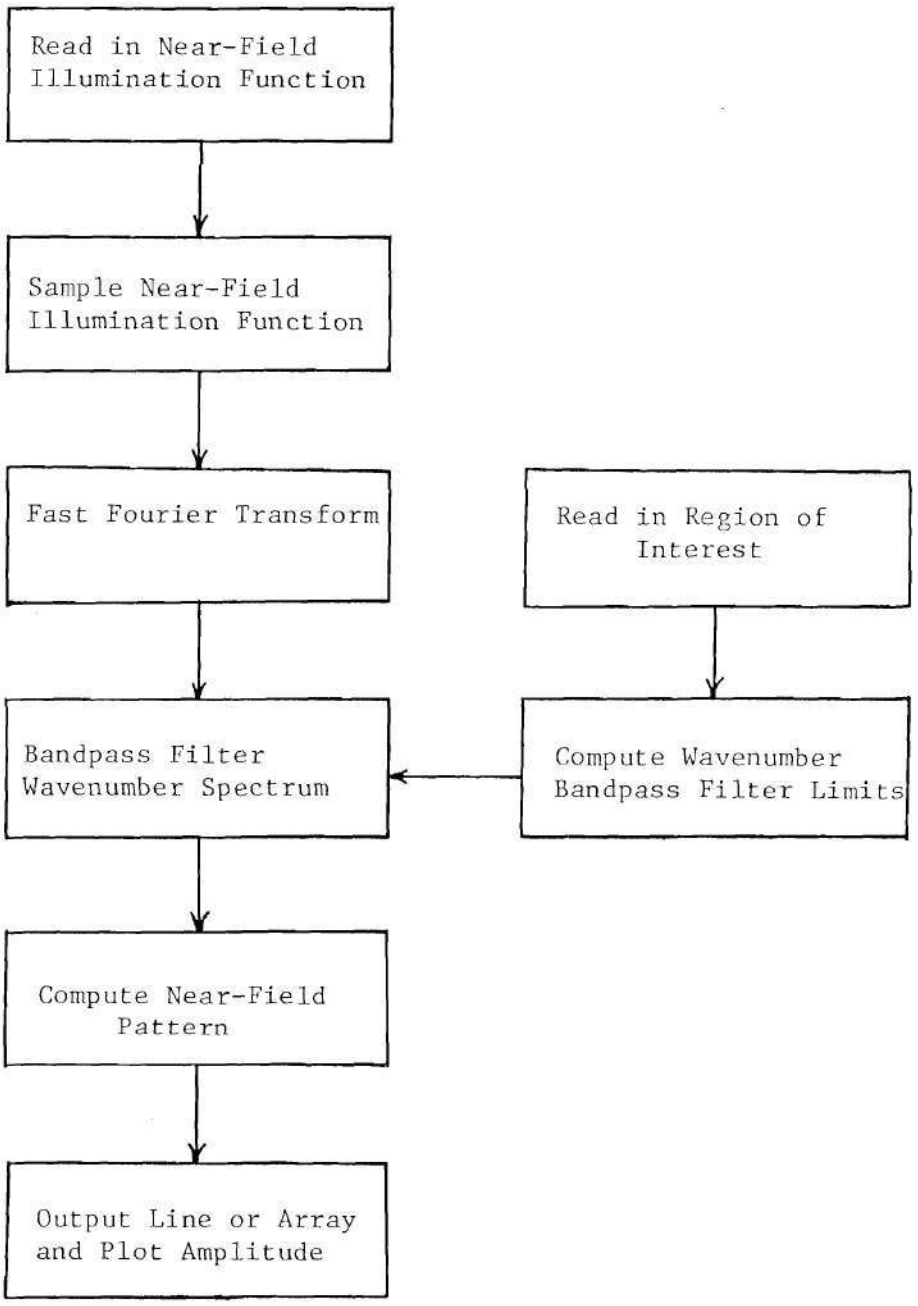

Figure 15. Block Diagram of the Computer Algorithm Near-field Computation Process.

is then sampled according to the wavenumber bandpass limits determined from Equations (19) and (20). The Bivariate integration quadrature is then employed to compute the near-zone fields in a particular region as a function of the distance (x) and angle of the observation point.

Computation of Near-Zone Fields

To test the algorithm, the near field of a uniformly illuminated 8λ square aperture was sampled in amplitude and phase over a 32λ by 32λ near-field plane as indicated in Figure 16. A sample spacing of $y = z = \lambda/2$ produces a 64 x 64 array of sampled near-field data points.

The center line ($k_y, k_z = 0$) of the plane wave spectrum computed using the discrete FFT from the sampled near field on the $x = 0$ plane of the uniformly illuminated 8λ square aperture is shown in Figure 17. The near field at range $x > 0$ was then obtained by integration of the PWS given in Equation (15) over the entire 64 x 64 plane wave spectrum array using the Bivariate integration algorithm. This integration corresponded to integration over all the visible wavenumbers (from $-k_o$ to $+k_o$). The calculated near-field pattern of the 8λ square aperture at a distance of $0.1\ D^2/\lambda$ is shown in Figure 18. Integration was also performed for the case of a uniformly illuminated 12λ (horizontal) by 6λ (vertical) rectangular aperture. The center line ($y, z = 0$) calculated near-field pattern is shown in Figure 19.

The integration, for a particular range, was also performed by using a wavenumber bandpass filter to solve

$$\bar{E}(x,y,z) = \frac{1}{2\pi} \int_{-k_{z(LP)}}^{+k_{z(LP)}} \int_{-k_{z(LP)}}^{+k_{y(LP)}} \bar{A}(k_y,k_z) e^{-j\bar{k}\cdot\bar{r}}\, dk_y dk_z , \qquad (58)$$

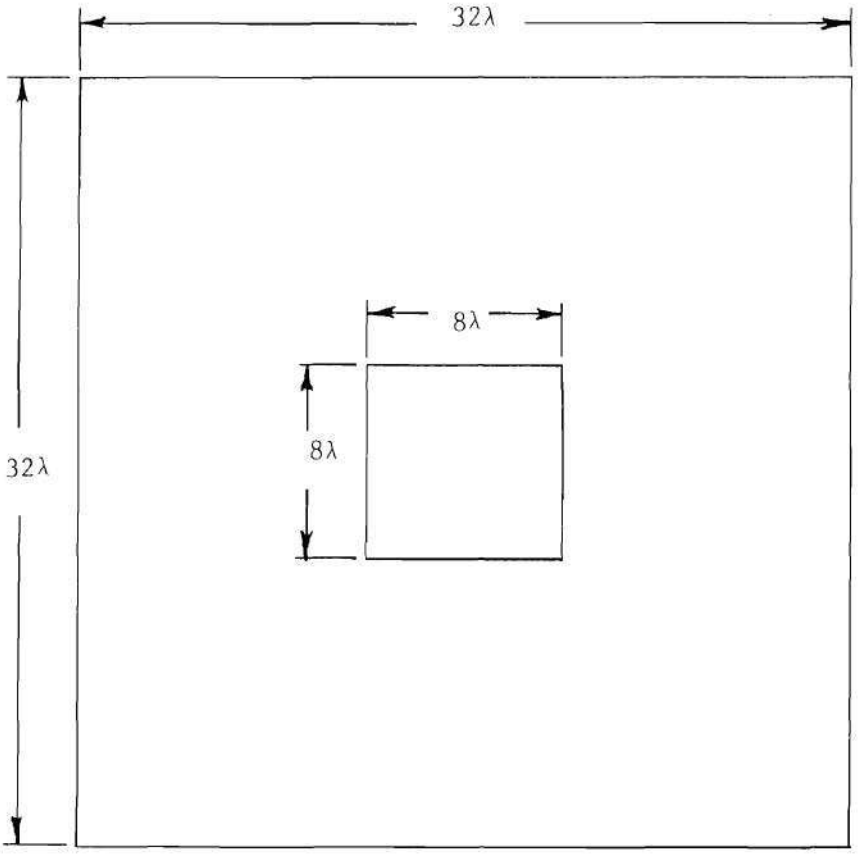

(a) Measurement Area

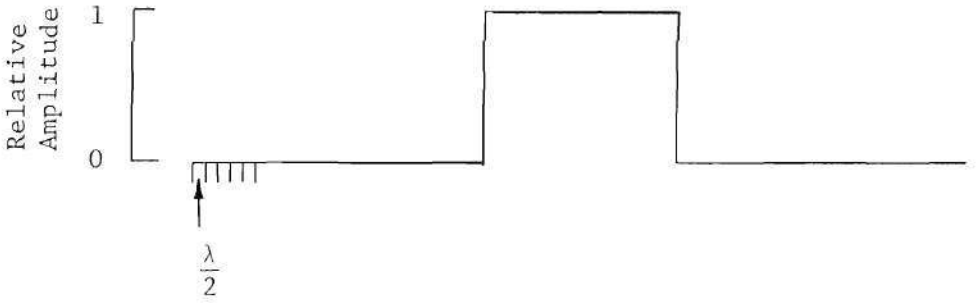

(b) Illumination Function and Sample Spacing

Figure 16. Location of Eight Wavelength Square Aperture in the Measurement Area and its Respective Illumination Function.

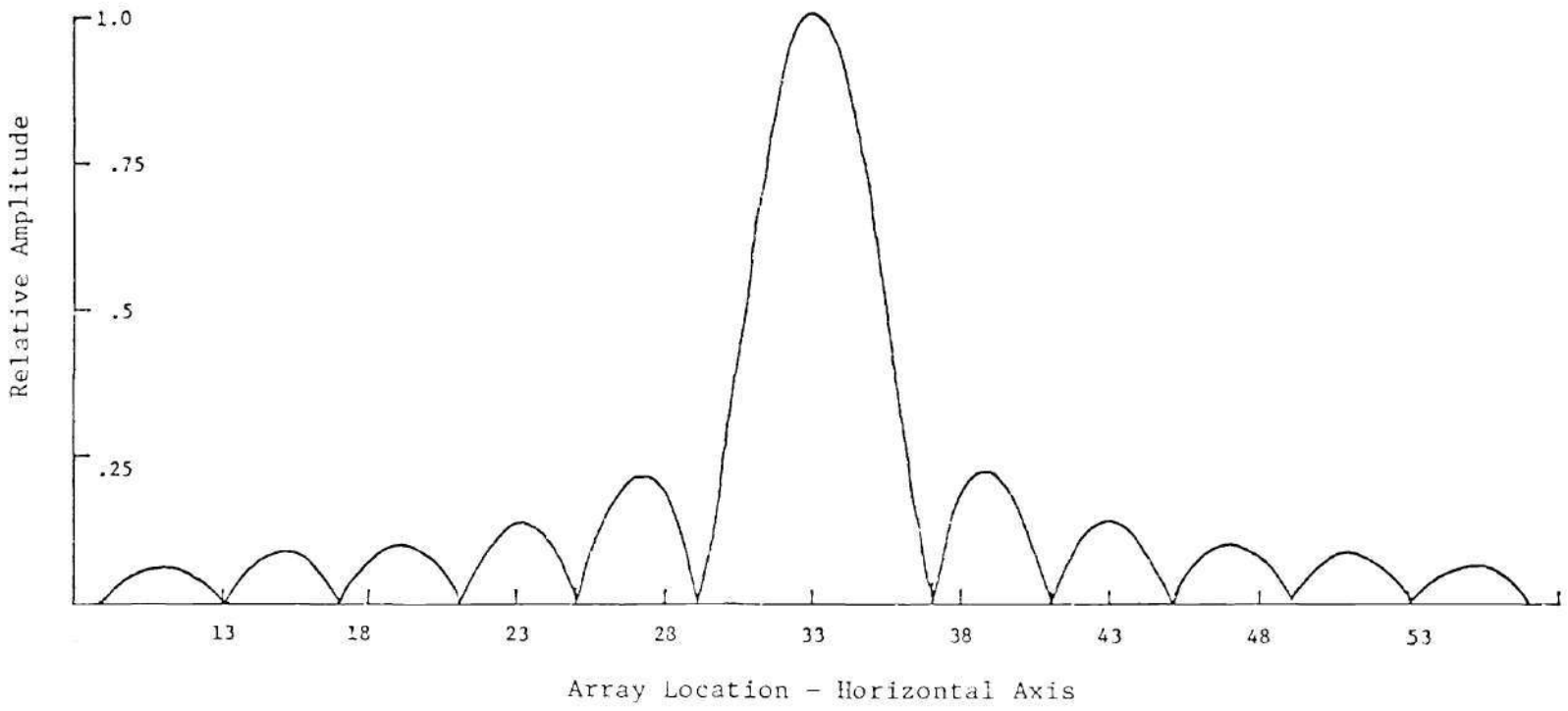

Figure 17. Magnitude of the Plane Wave Spectrum of the Transformed Near-field Data Along a Horizontal Line Through the Vertical Center of the Measured Array.

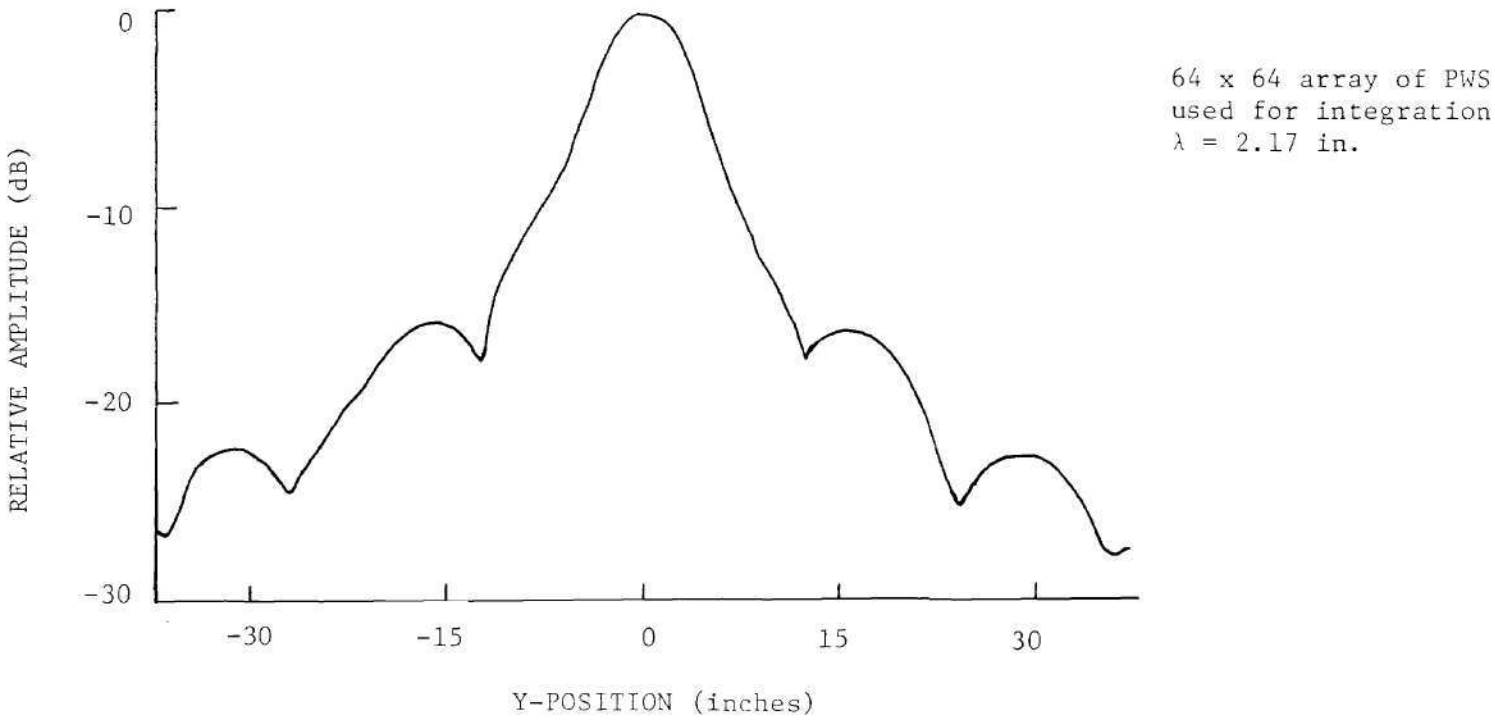

Figure 18. Computed Near Field of a Uniformly Illuminated 8-Wavelength Square Aperture Using Visible Wavenumber Spectrum at a Near-field Distance of 6.44 Wavelengths (z=0).

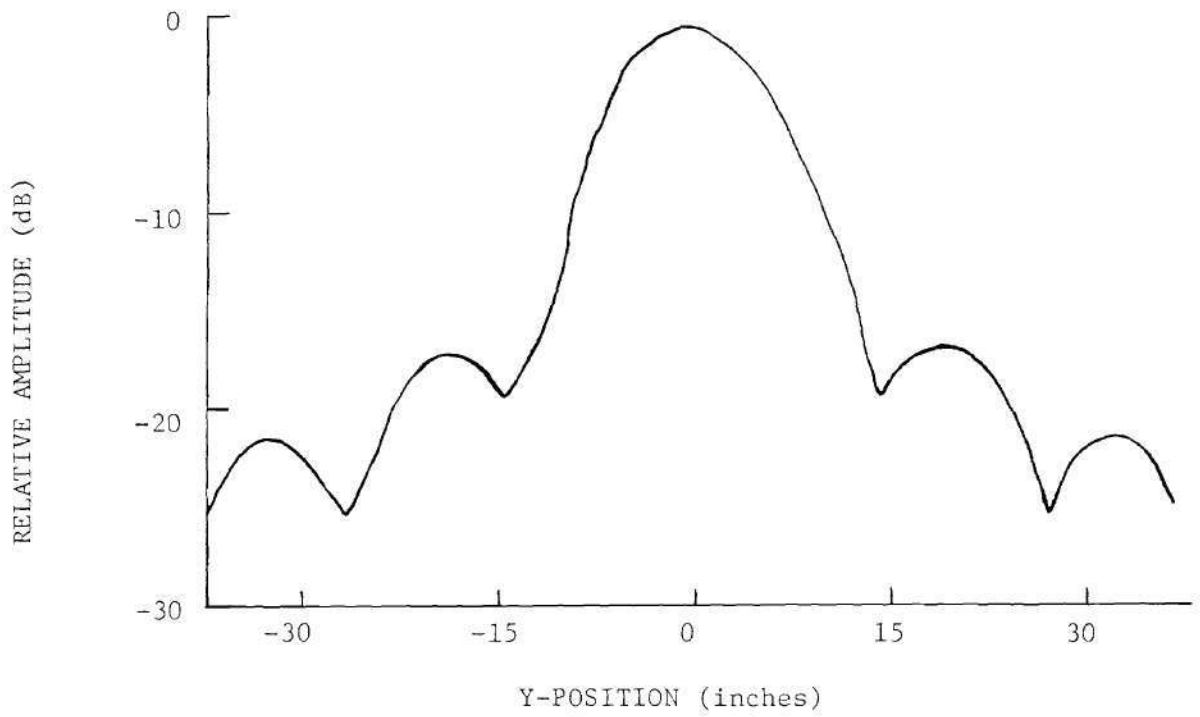

Figure 19. Computed Near Field of a Uniformly Illuminated 12-Wavelength by 6-Wavelength Rectangular Aperture Using Visible Wavenumber Spectrum at a Near-field Distance of 12.8 Wavelengths (z=0).

where

$$\bar{k} \cdot \bar{r} = \sqrt{k_o^2 - k_y^2 - k_z^2}\ x + k_y y + k_z z \ ,$$

from minus $.188k_o$ to plus $.188k_o$ which corresponds to a 12 x 12 array centered about $k_y = k_z = 0$ in the wavenumber spectrum. The results obtained from the integration over the wavenumber band-limited region are shown in Figure 20.

The near-field patterns computed using the wavenumber bandpass filtering concept are compared to near-field patterns computed from unfiltered spectral data and aperture integration in Chapter IV.

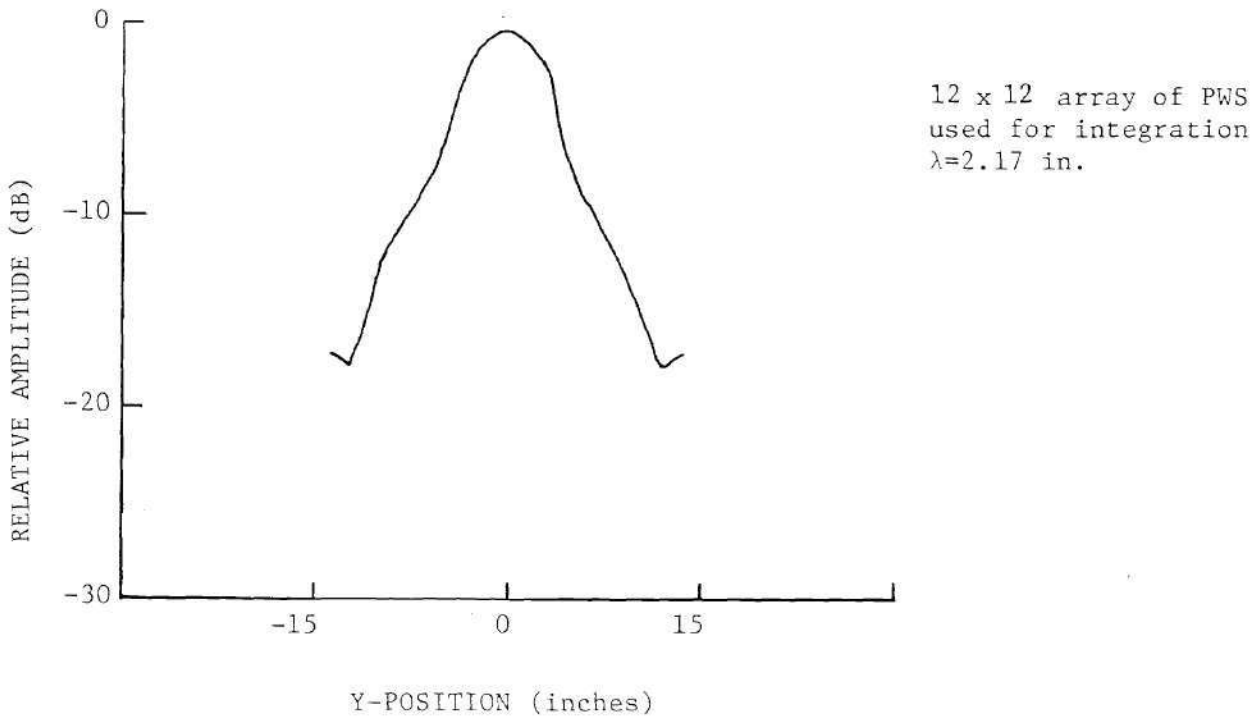

Figure 20. Comparison of the Calculated Near Fields of a Uniformly Illuminated 8λ Square Aperture Using Band-pass Filtered and Unfiltered Spectral Data at a Near-field Distance of 6.44 Wavelengths (z=0).

CHAPTER IV

RESULTS

In this chapter, the results of the near-zone radiation patterns computed using the plane wave spectrum approach are presented. The near-zone patterns computed from bandpass filtered spectral data are compared to near-zone patterns computed from unfiltered PWS data and to near-zone patterns computed using aperture field integration techniques. Further, a comparison of the amount of spectral data and computation time required to compute the near-zone patterns using wavenumber filtered and unfiltered spectral data is presented.

The Bivariate integration algorithm described in Chapter III was employed to compute near-field patterns using a known and entire visible wavenumber spectrum and to compute wavenumber bandpass filtered patterns for two near-field distances. In each case, solutions to the integral of Equation (58) were obtainable.

Integrating the PWS of the uniformly illuminated 8λ square aperture from minus $0.250\ k_o$ to plus $0.250\ k_o$, which corresponds to a 16 by 16 array centered about $k_y = k_z = 0$ in the wavenumber spectrum, yields the results shown in Figure 21. In this figure only the center line data representing a single near-field "cut" is plotted, and good agreement between the wavenumber band-limited and full spectrum computations is obtained over the main beam and first sidelobe regions.

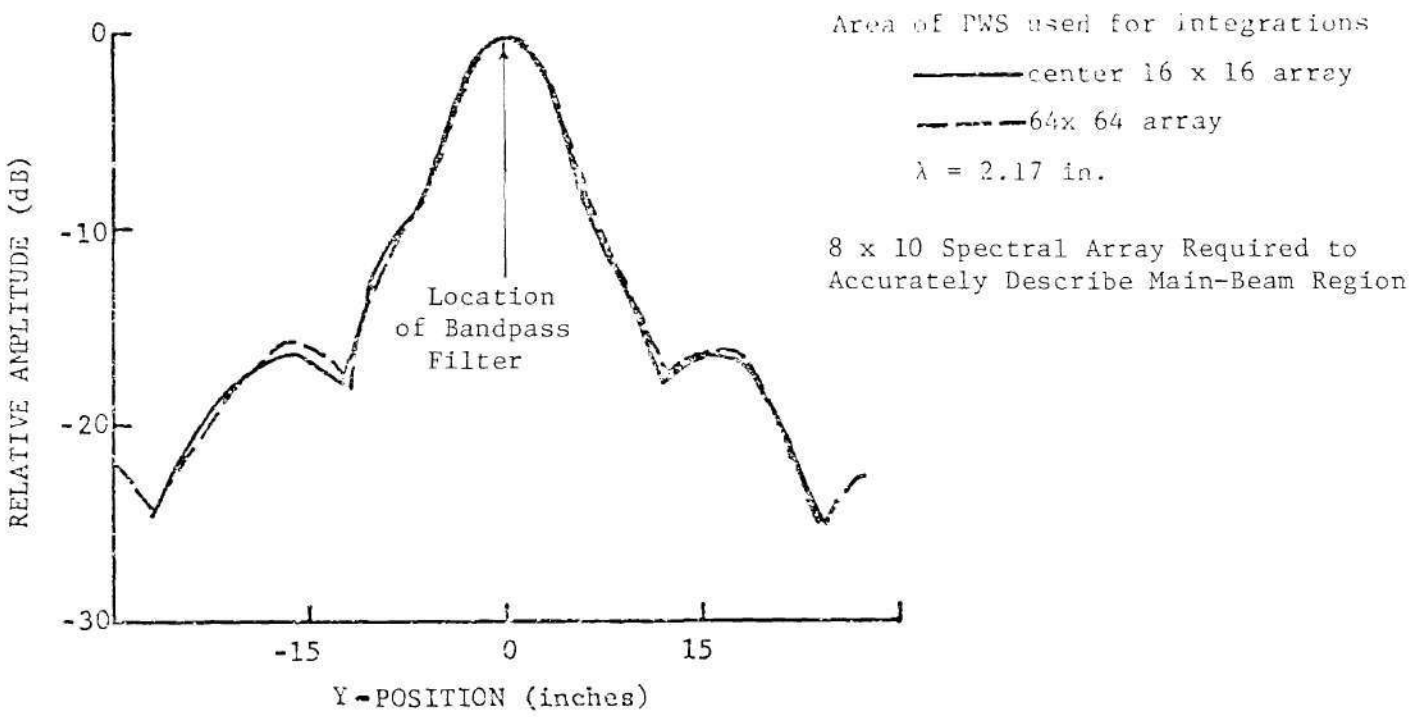

Figure 21. Comparison of the Calculated Near Field of a Uniformly Illuminated 8-Wavelength Square Aperture Using a 16 x 16 Band-pass Filtered and a 64 x 64 Unfiltered Plane Wave Spectrum at a Near-field Distance of 6.44 Wavelengths.

The results of the quasi-optics technique from Chapter II given by Equations (19) and (20) indicate that a minimum array of 8 x 10 spectral samples are required to represent the significant spectrum contributions to the main-beam region fields. Employing a wavenumber bandwidth which encloses a larger region than required only increases the effective size of the near-field sector over which accurate numerical results are obtained. For the case where eight spectral samples are required to accurately determine the near-field pattern over the main beam region, integration over a 16 x 16 wavenumber array results in good agreement in both the main beam and first sidelobe regions of Figure 21. The results of bandpass filtering the wavenumber region to $0.250\ k_o$, which corresponds to integration over an 8 x 8 array of spectral samples, are shown in Figure 22. Here, the near field computed from the bandpass filtered PWS is compared to the near field computed using the unfiltered 64 x 64 PWS. Again, very good agreement is exhibited in the main-beam region with minor discrepancies appearing in the first sidelobe. Therefore, it could be said that Equations (19) and (20) provide an accurate first order estimate of the size of the spectral region required to describe a particular sector of interest, at least in the main-beam region. Figure 23 and Figure 24 indicate the results of integration over a 6 x 6 array and 4 x 4 array of spectral samples, respectively. In these cases, the size of the wavenumber limited region was not large enough to describe the main beam, but good agreement with the boresight amplitude was maintained. From these results, one can see that errors tend to increase gradually as the size of the wavenumber region is decreased. In addition, it is also evident that as a

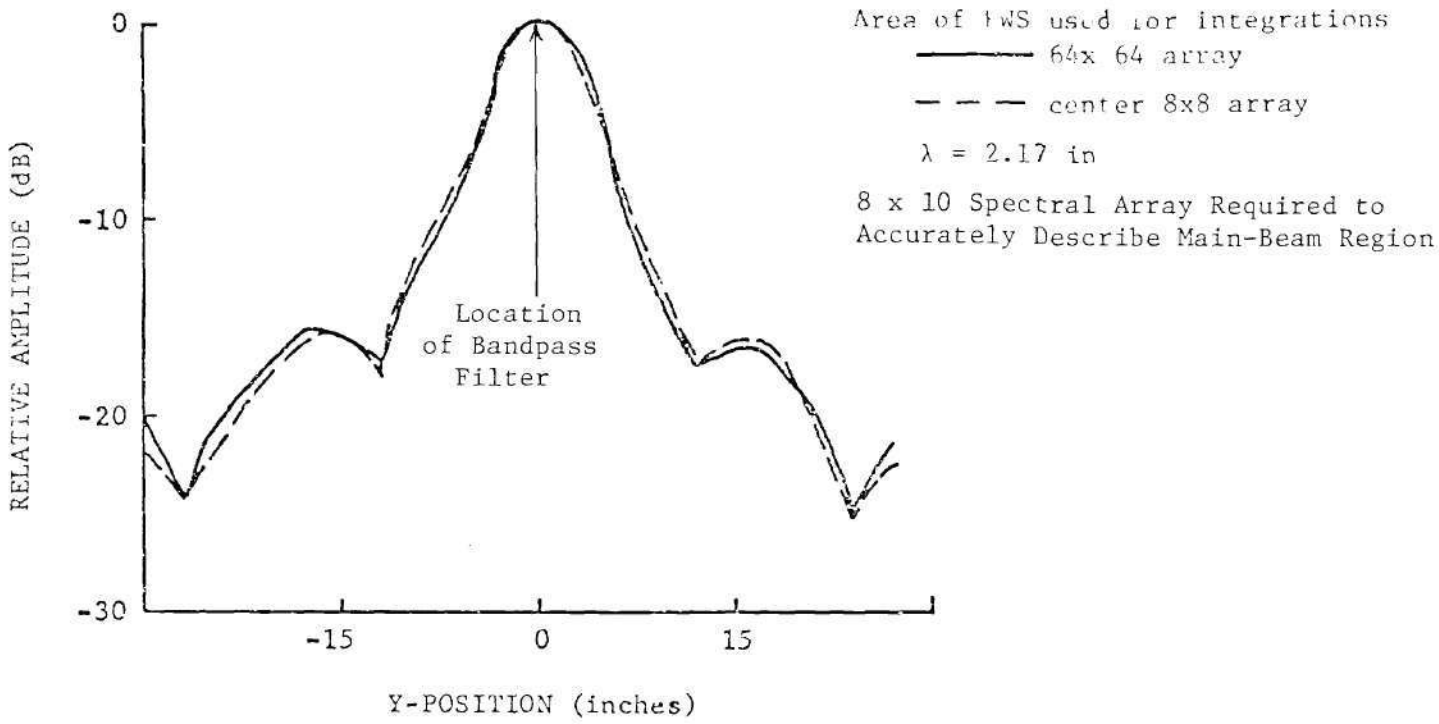

Figure 22. Comparison of the Calculated Near Field of a Uniformly Illuminated 8-Wavelength Square Aperture Using a 8 x 8 Band-pass Filtered and a 64 x 64 Unfiltered Plane Wave Spectrum at a Near-field Distance of 6.44 Wavelengths.

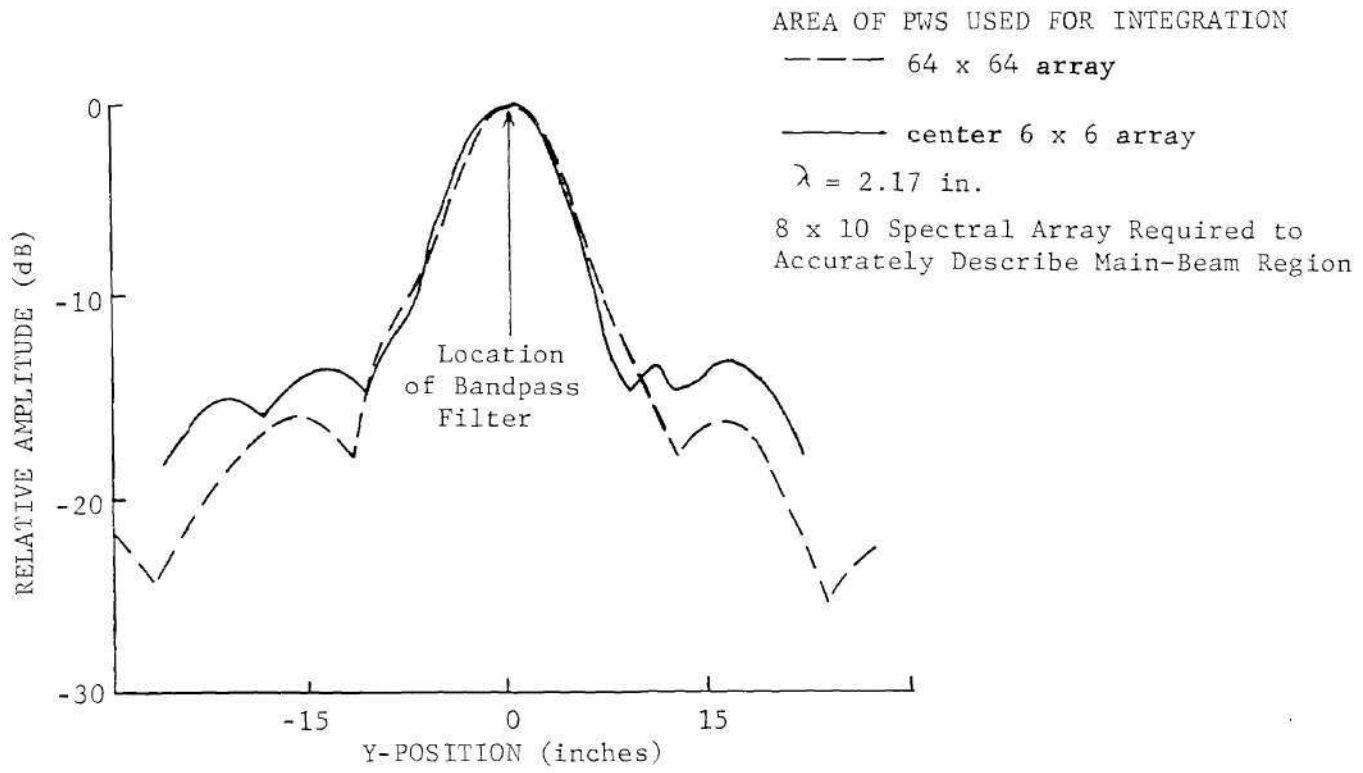

Figure 23. Comparison of the Calculated Near Field of a Uniformly Illuminated 8-Wavelength Square Aperture using a 6 x 6 Band-pass Filtered and a 64 x 64 Unfiltered Plane Wave Spectrum at a Near-field Distance of 6.44 Wavelengths.

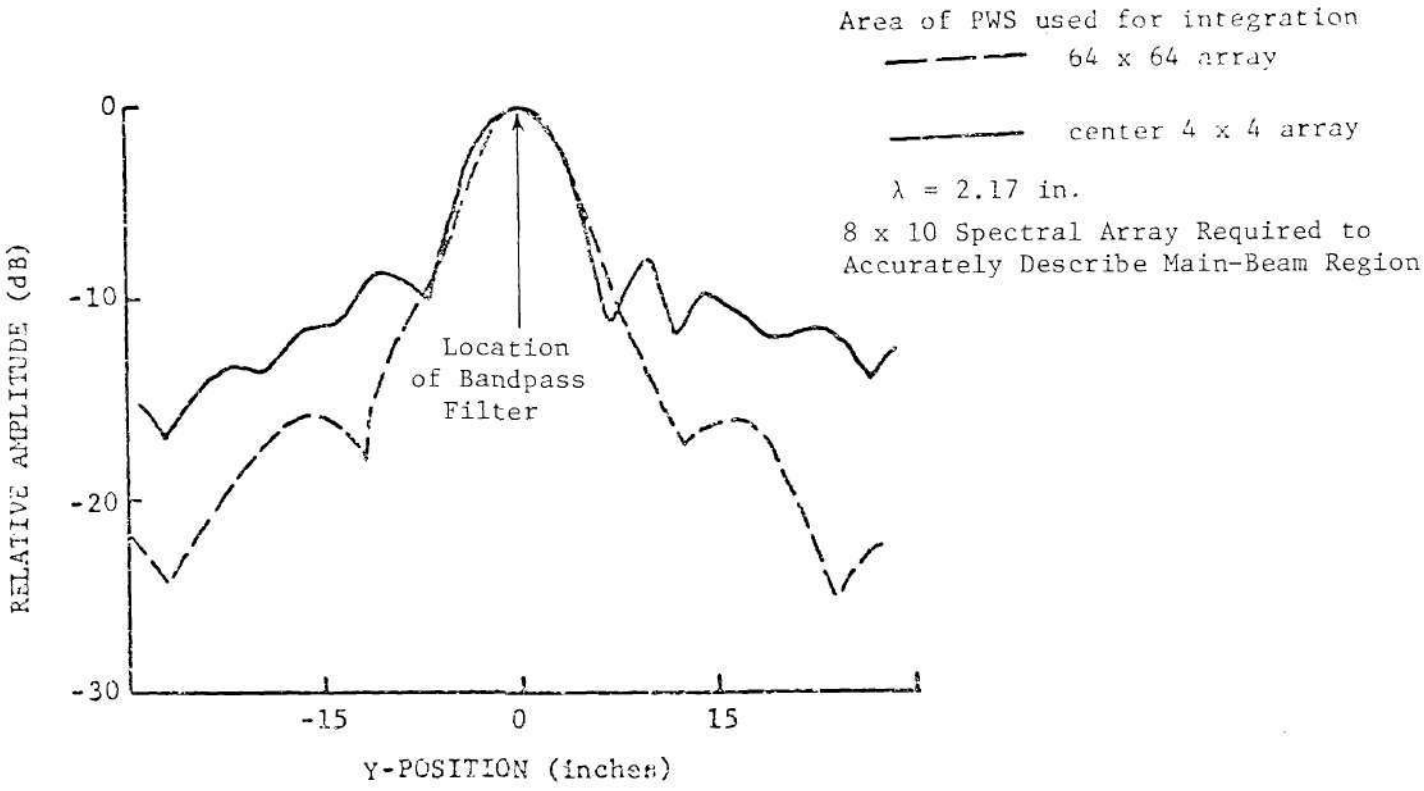

Figure 24. Comparison of the Calculated Near Field of a Uniformly Illuminated 8-Wavelength Square Aperture Using a 4 x 4 Band-pass Filtered and a 64 x 64 Unfiltered Plane Wave Spectrum at a Near-field Distance of 6.44 Wavelengths.

reduction in the number of included spectral samples is made, the wavenumbers which describe the main beam region do not accurately describe the first sidelobe region.

In Figure 25, the near field computed using the plane wave spectrum method over the visible wavenumber region is compared to the near field computed using aperture integration techniques. As indicated in Figure 25, very good agreement exists between the two integration techniques, especially over small angles from the boresight axis. Figures 26 and 27 present the results of wavenumber limiting for a near-field distance of $0.05D^2/\lambda$, and the results again demonstrate the effectiveness of waveband limiting. Figure 28 compares the near field computed over a 32 x 32 wavenumber array ($-0.5k_o$ to $+0.5k_o$) using the PWS method to the near field computed using aperture field integration for a distance of 3.22 wavelengths from the aperture.

As previously discussed, if the angular region of interest is a region other than the center, bandpass filtering can be used to compute the significant field contributions in that region. Figure 29(b) indicates the spectral region used to calculate the field in the first sidelobe near-field region using a 16 x 16 wavenumber array. The results of the wavenumber limiting in the sidelobe region are presented in Figure 30 for calculations along the center-line path indicated in Figure 29(a). Equations (19) and (20) from Chapter II indicate a spectral region corresponding to a 10 x 12 wavenumber array is required to accurately describe the near field in the first sidelobe region. The good agreement of the results in the first sidelobe region indicates that the

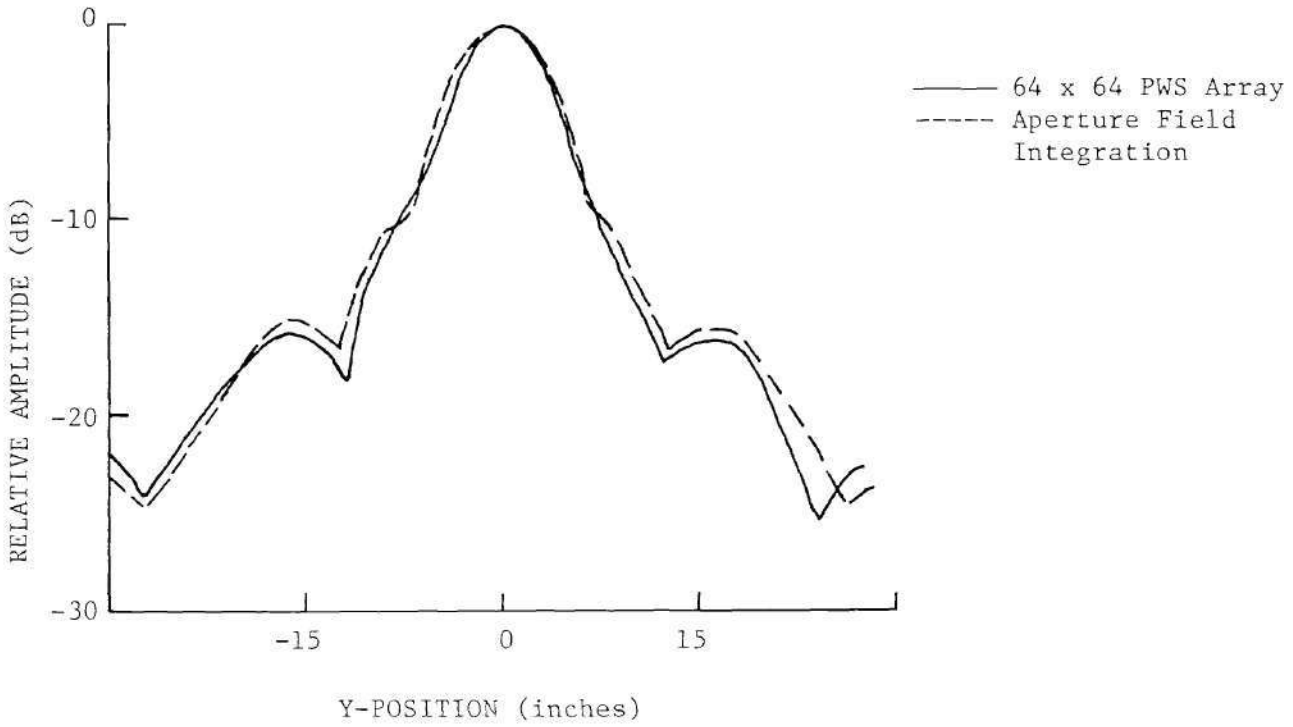

Figure 25. Comparison of the Calculated Near Field of a Uniformly Illuminated 8-Wavelength Square Aperture Using PWS and Aperture Integration Techniques at a Near-field Distance of 6.44 Wavelengths.

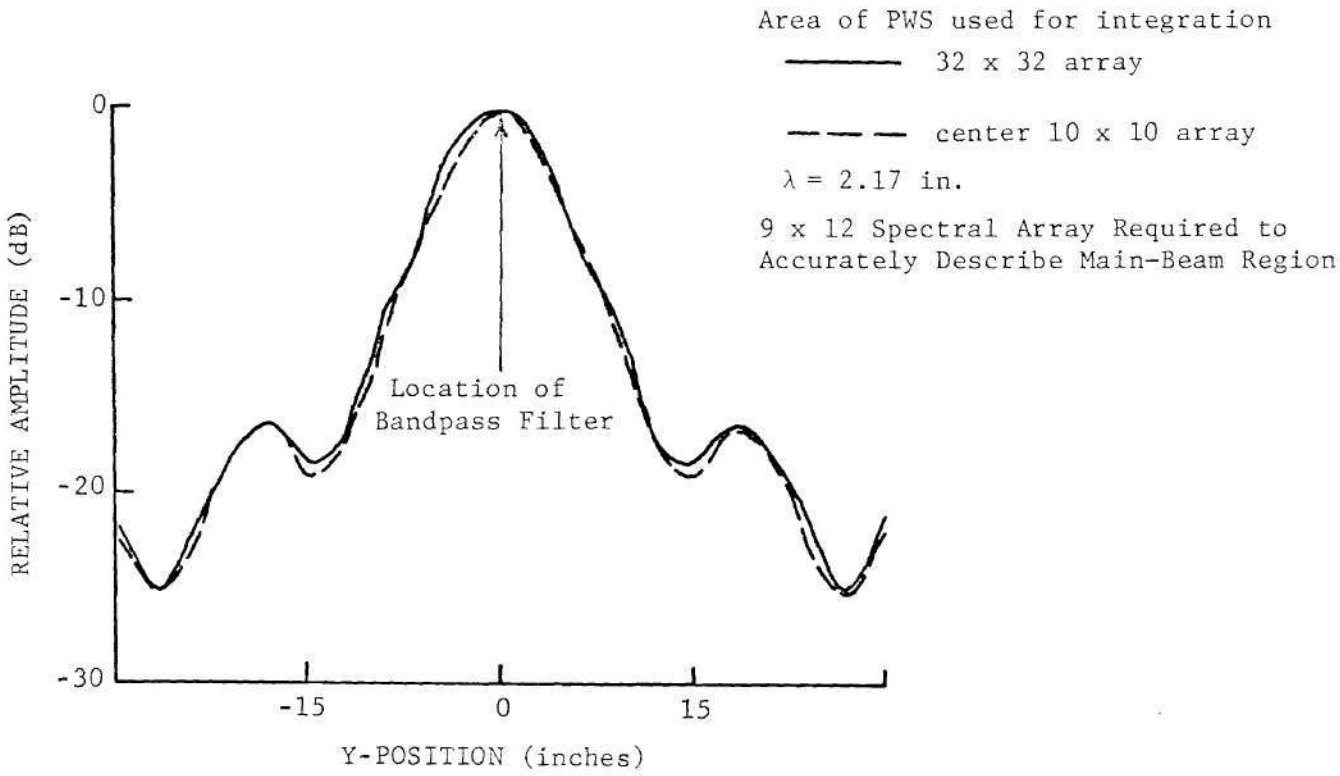

Figure 26. Comparison of the Calculated Near Field of a Uniformly Illuminated 8-Wavelength Square Aperture Using a 10 x 10 Band-pass Filtered and a 32 x 32 Unfiltered Plane Wave Spectrum at a Near-field Distance of 3.22 Wavelengths.

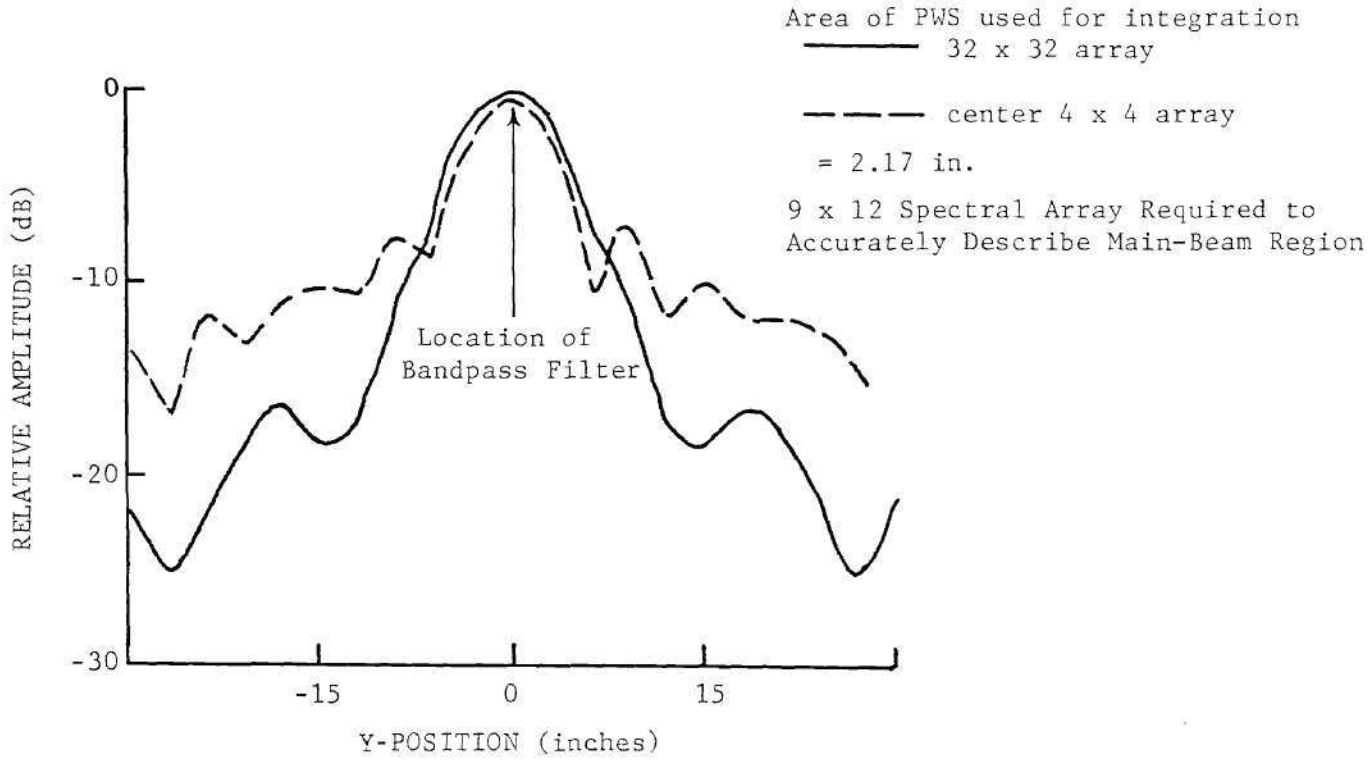

Figure 27. Comparison of the Calculated Near Field of a Uniformly Illuminated 8-Wavelength Square Aperture Using a 4 x 4 Band-pass Filtered and a 32 x 32 Unfiltered Plane Wave Spectrum at a Near-field Distance of 3.22 Wavelengths.

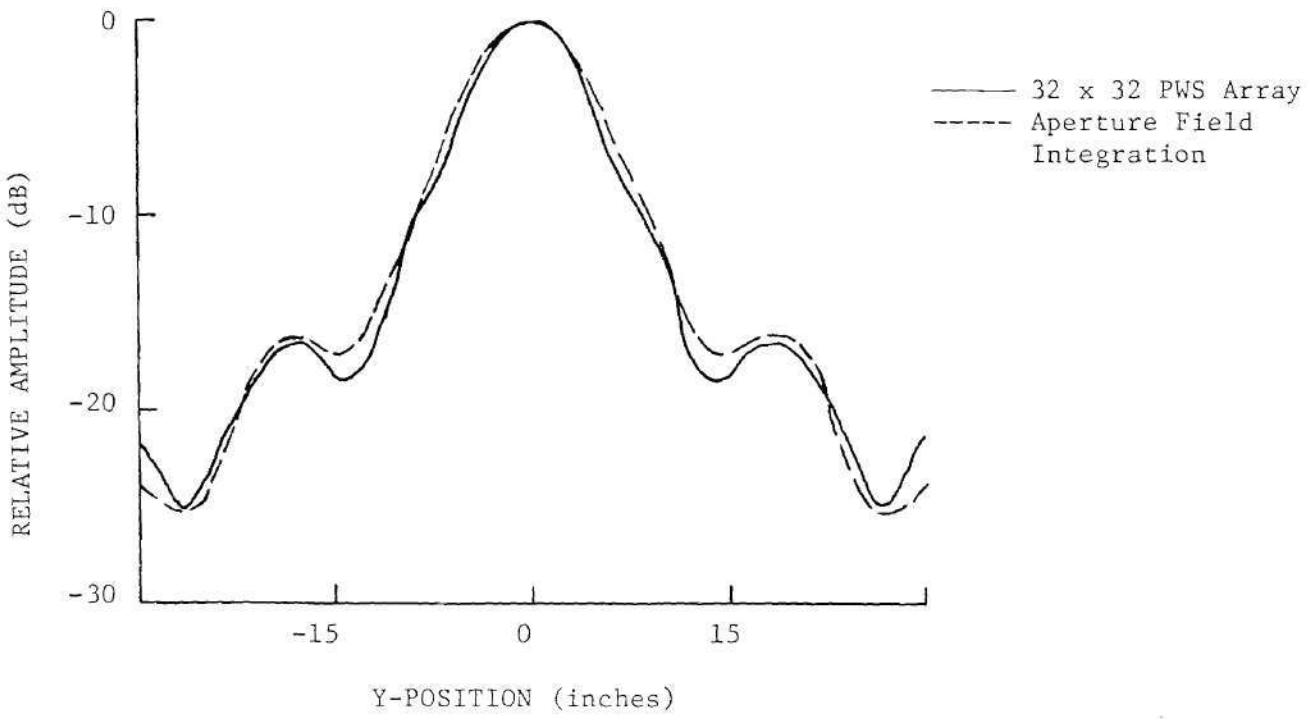

Figure 28. Comparison of the Calculated Near Field of a Uniformly Illuminated 8-Wavelength Square Aperture Using PWS and Aperture Integration Techniques at a Near-field Distance of 3.22 Wavelengths.

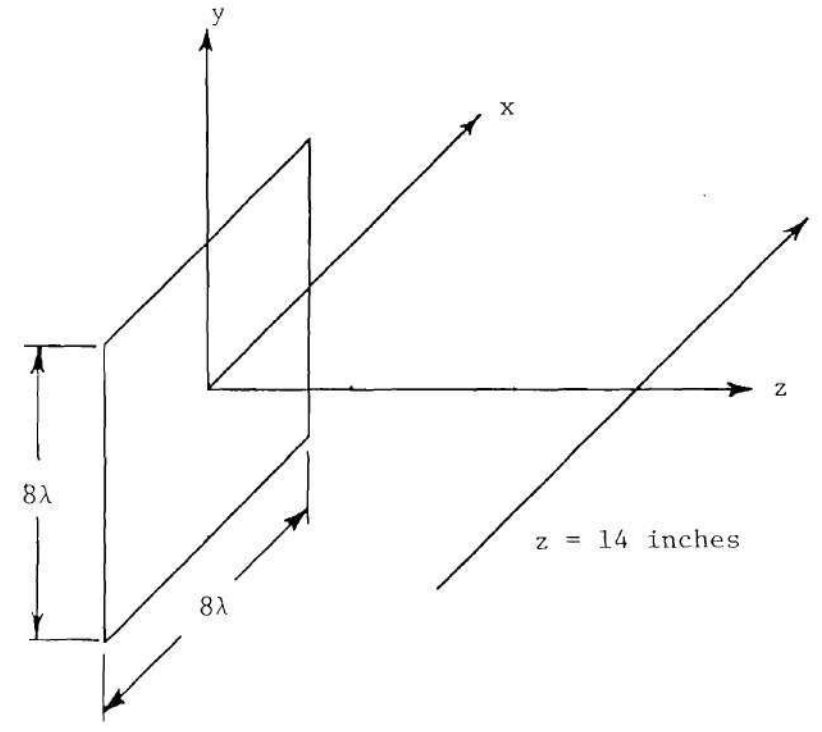

(a)

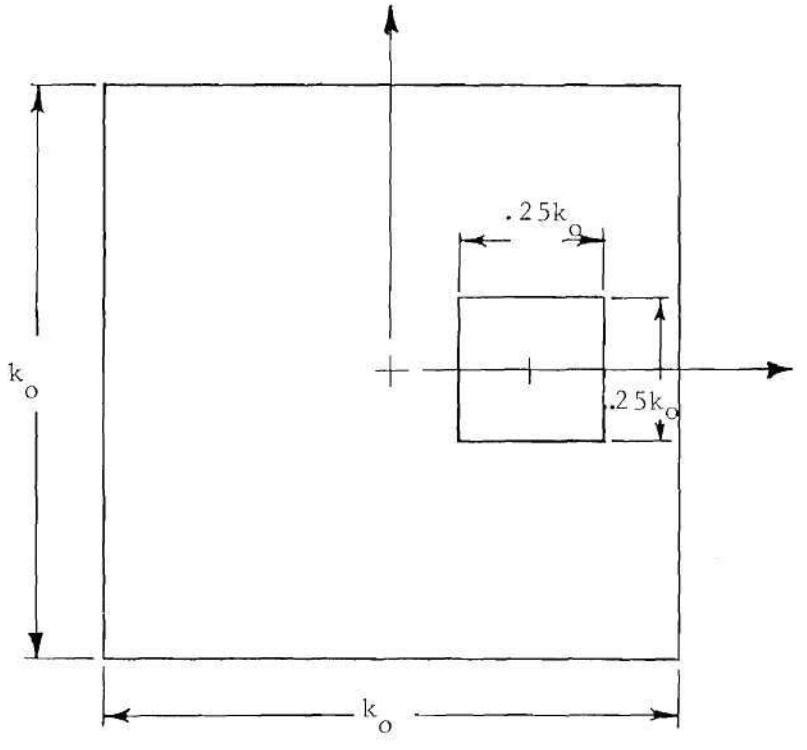

(b)

Figure 29. (a) Illustration of Path Used for Near-field "Flyby" Calculations at a Measurement Distance of 6.44λ and (b) Band-pass Filtered Wavenumber Region of Spectral Data Used for Calculation of First Sidelobe.

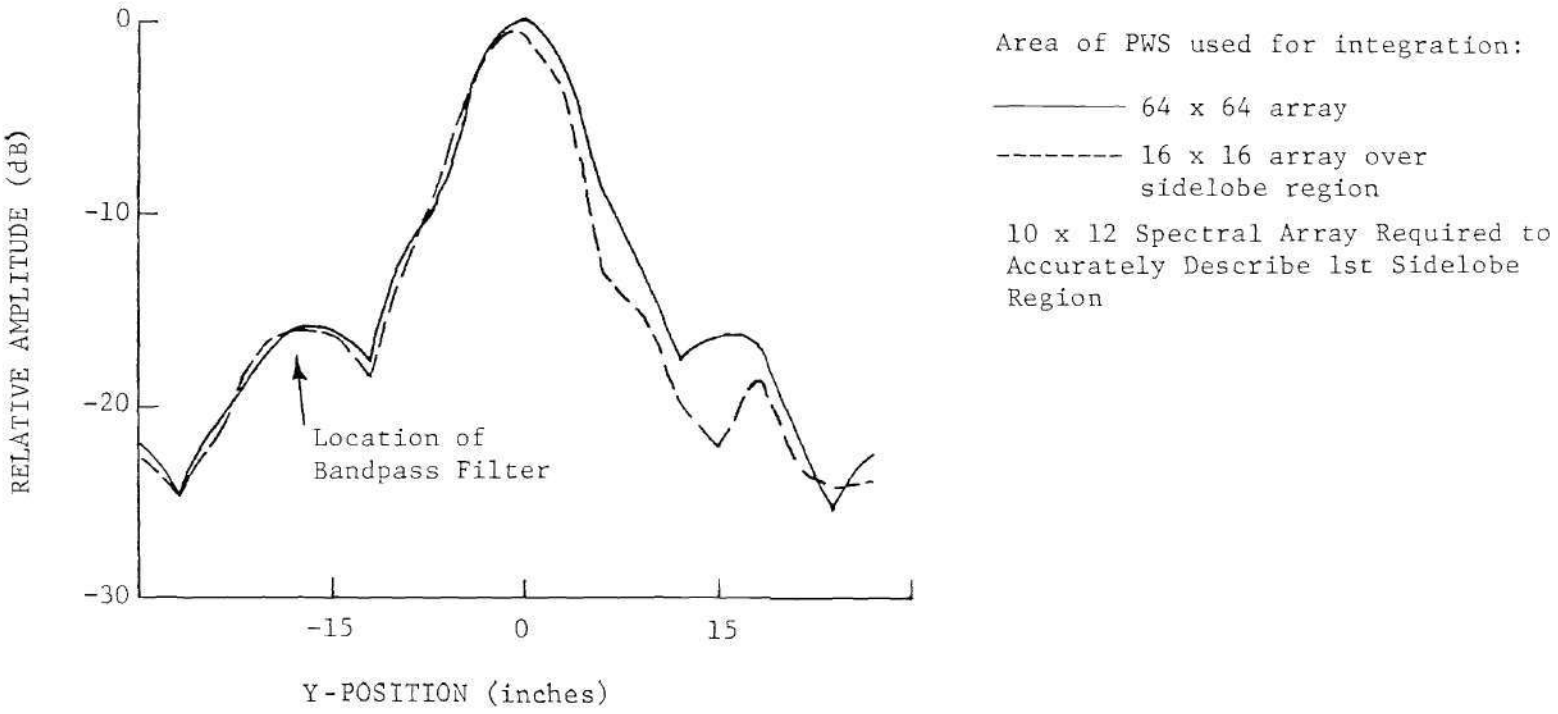

Figure 30. Comparison of the Calculated Near Field of a Uniformly Illuminated 8-Wavelength Square Aperture Using a 16 x 16 Band-pass Filtered and a 64 x 64 Unfiltered Plane Wave Spectrum. The 16 x 16 Band-pass Filtered Spectrum is Located at the First Sidelobe Region and the Near-field Distance is 6.44 Wavelengths.

size of the wavenumber region used to describe the near field in the region of interest can be significantly reduced and still provide an accurate description of the field in that region. Figure 31 presents the results of integration over a smaller 8 x 8 wavenumber array centered on the sidelobe, and reasonably good agreement is obtained in the sidelobe region for this small wavenumber array. These results demonstrate that wavenumber band-limiting is an effective and useful technique for near-field computation.

A larger 16-wavelength aperture was also examined to determine the effect of including an erroneous bandpass region. Figure 32 compares a 64 x 64 wavenumber array to a bandpass filtered 4 x 4 wavenumber array which contains the predicted number of spectral samples required to accurately describe the main beam region. It can be seen that for this larger aperture good agreement is obtained in the main beam region, but not in the first sidelobe. Moving the spectral window to the region defined by the angular position of the first sidelobe yields the results shown in Figure 33. In this case, good agreement is seen in the first sidelobe region.

Based on the results presented in Figures 21-24, one notes that as the size of the spectral region used to compute an angular sector of interest is reduced, the errors increase gradually. Figures 32 and 33 indicate that the location of the spectral window does indeed depend upon the angular location of the near-field sector of interest.

The computation of the integral of Equation (15) employing numerical integration techniques is proportional to the number of lobes of the integrand. Sixteen integration points per square wavelength were

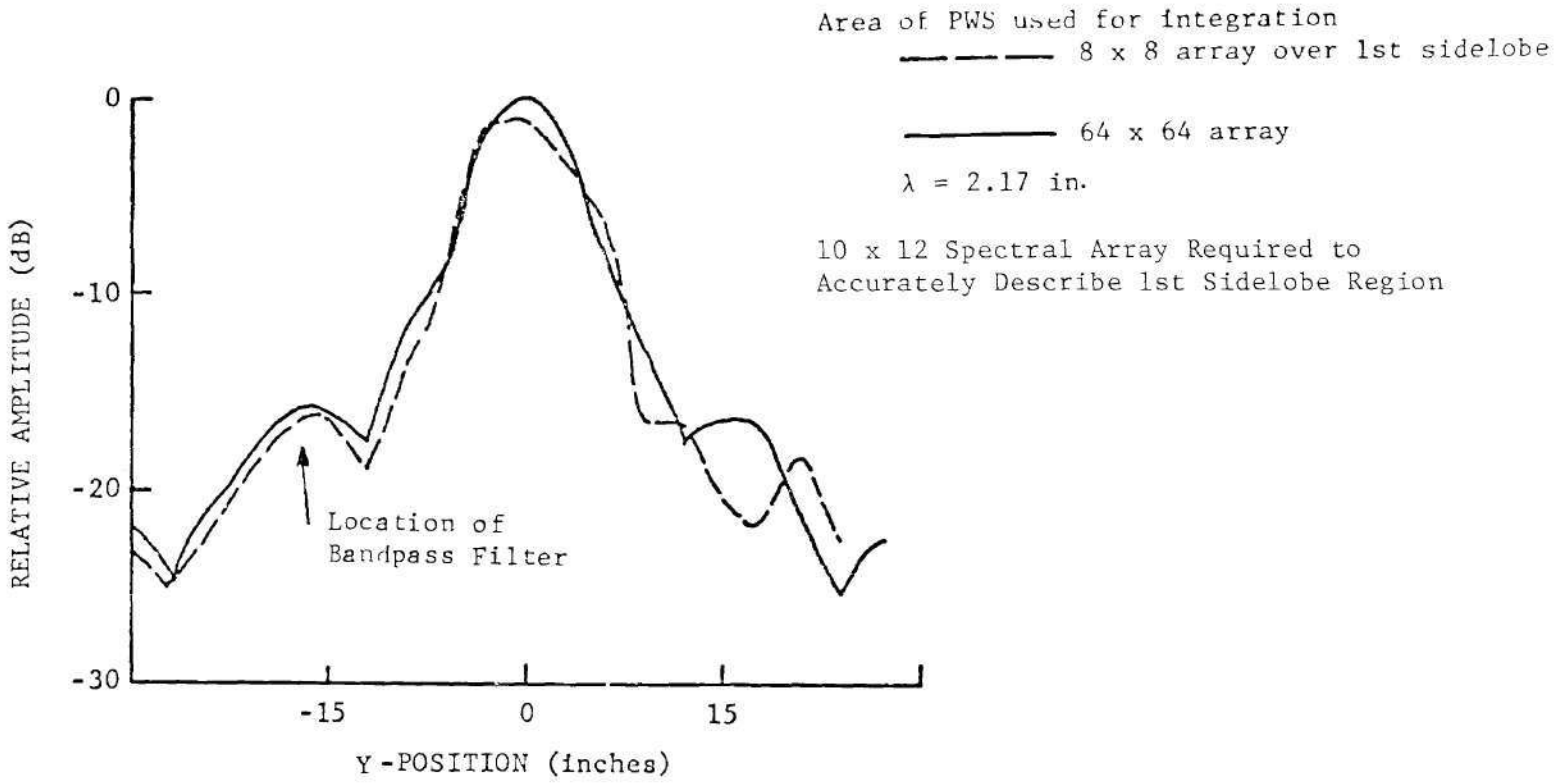

Figure 31. Comparison of the Calculated Near Field of a Uniformly Illuminated 8-Wavelength Square Aperture Using a 8 x 8 Band-pass Filtered and a 64 x 64 Unfiltered Plane Wave Spectrum. The 8 x 8 Band-pass Filtered Spectrum is Located at the First Sidelobe Region and the Near-field Distance is 6.44 Wavelengths.

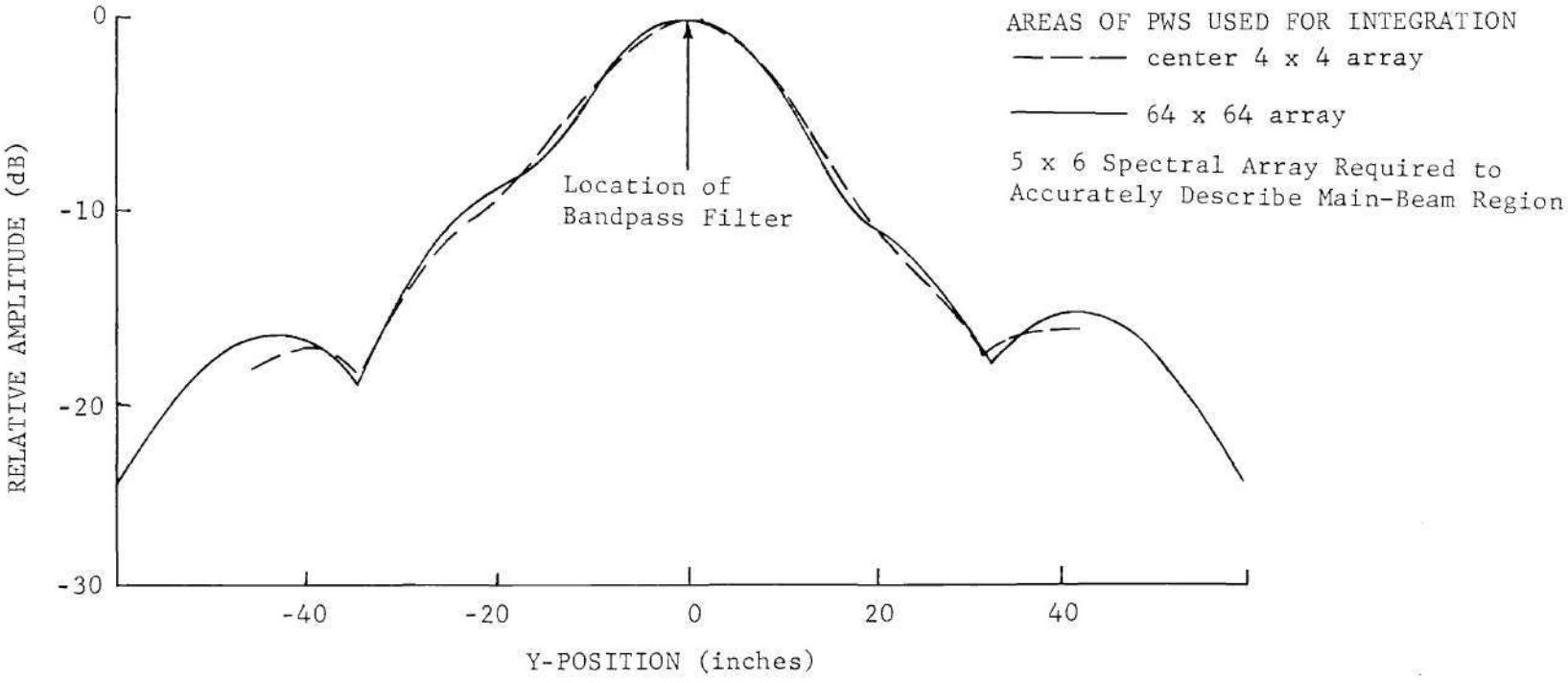

Figure 32. Comparison of the Calculated Near Field of a Uniformly Illuminated 16-Wavelength Square Aperture Using a 4 x 4 Band-pass Filtered and a 64 x 64 Unfiltered Plane Wave Spectrum at a Near-field Distance of 20.48 Wavelengths.

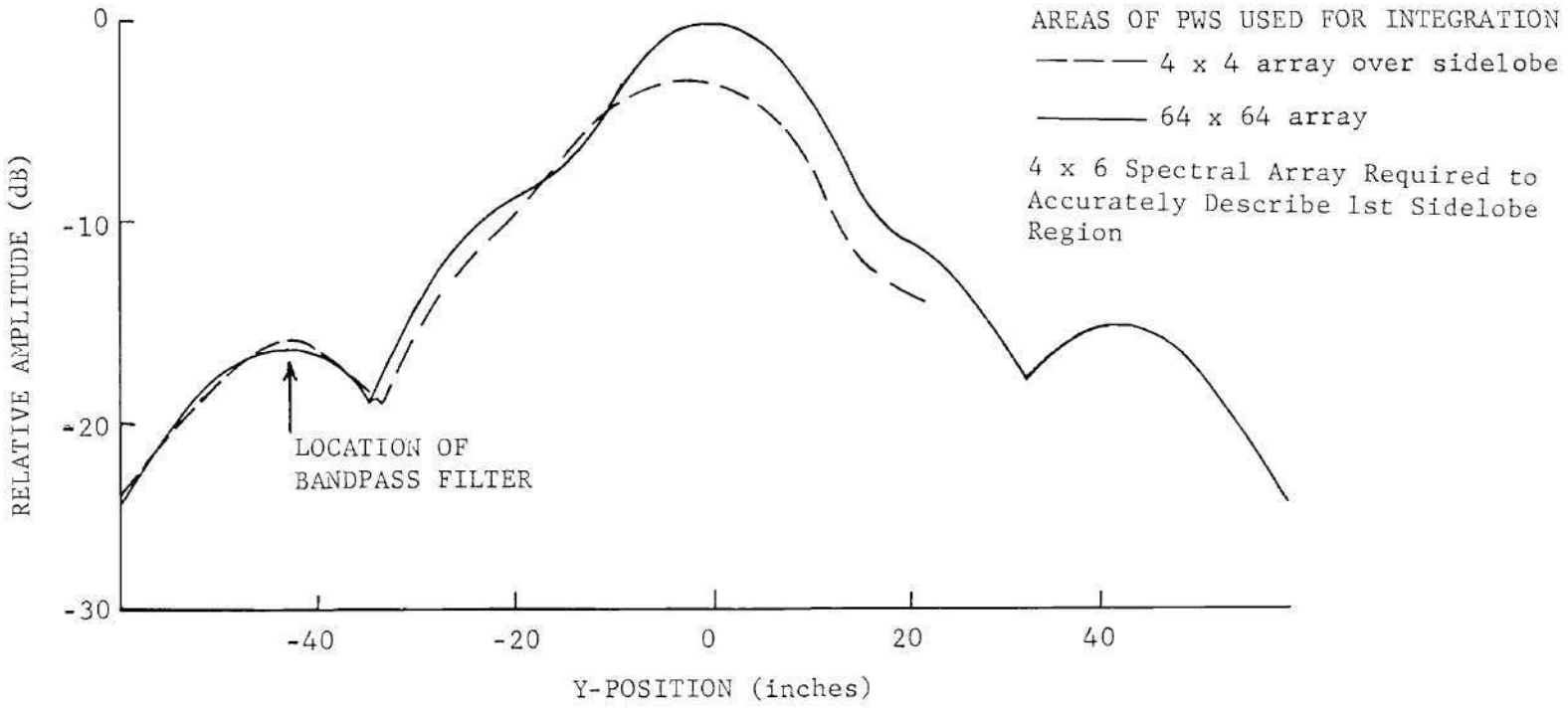

Figure 33. Comparison of the Calculated Near Field of a Uniformly Illuminated 16-Wavelength Square Aperture Using a 4 x 4 Band-pass Filtered and a 64 x 64 Unfiltered Plane Wave Spectrum. The 4 x 4 Band-pass Filtered Spectrum is Located at the First Sidelobe Region and the Near-field Distance is 20.48 Wavelengths.

used to compute each field point using the aperture field integration method. The number of integration points used for the PWS method was dependent upon the size of the wavenumber region used as determined by Equations (19) and (20). In Table 1, the computation times required for the results presented previously are listed. Significant improvement in computation time over the PWS method without filtering is observed for cases where wavenumber bandpass filtering was used. In cases where accurate near-field results were obtained, the reduction in computation time ranged from approximately a factor of five to a factor of seventeen. Table 2 compares computation times for the aperture field integration, unfiltered PWS, and wavenumber bandpass filtered PWS methods. For an 8-wavelength square aperture, the improvement of the unfiltered PWS method over aperture field integration is only 1.16. Yet for a 50-wavelength aperture, a factor of 57.9 improvement over aperture integration is obtained using the PWS method. For the 16λ aperture of Figures 32 and 33 a factor of 4.6 improvement over aperture integration is obtained even when the entire visible PWS is used. However, significant reduction in computation time can also be achieved for small apertures when wavenumber bandpass filtering is used. Table 2 indicates up to a factor of 20 improvement for cases where accurate near-field results were obtained.

As seen from the results presented in this chapter, errors caused by using wavenumber bandwidths which enclose too small a region tend to increase gradually. Obviously, optimum choices of wavenumber bandwidth and location will result in the greatest accuracy and shortest computation

Table 1. Comparison of Computation Times for Wavenumber Filtered and Unfiltered PWS (8λ Square Aperture)

Figure Number	Number of Points Computed	Area of PWS Used For Integration	Time (secs) Unfiltered PWS	Filtered PWS	Ratio
18	40	$-k_o$ to $+k_o$	152	---	---
21	20	$-.25\ k_o$ to $+.25\ k_o$	76	12.9	5.5
22	30	$-.125\ k_o$ to $+.125\ k_o$	114	6.5	17.5
23	30	$-.0938\ k_o$ to $+.0938\ k_o$	114	4.9	23.2
24	20	$-.0625\ k_o$ to $+.0625\ k_o$	76	2.8	27.1
26	20	$-.140\ k_o$ to $+.140\ k_o$	76	5.6	13.6
27	20	$-.0625\ k_o$ to $+.0625\ k_o$	76	2.9	26.2
30	20	$+.125\ k_o$ to $+.625\ k_o$	76	14.1	5.4
31	20	$+.25\ k_o$ to $+0.5\ k_o$	76	4.9	15.5

time. Employing a larger wavenumber bandwidth than is required only slightly improves accuracy in a particular region of interest, but could significantly increase computation time.

Table 2. Comparison of Computation Times for PWS and Aperture Field Methods (8λ Square Aperture)

Number of Points Computed	Area of PWS Used for Integration	Time (sec) AFI	PWS	Ratio
40	Aperture Field	176	---	---
40	$-k_o$ to $+k_o$	176	152	1.16
30	$-.5\ k_o$ to $+.5\ k_o$	132	76.4	1.73
20	$-.25\ k_o$ to $+.25\ k_o$	88	14.2	6.20
30	$-.125\ k_o$ to $+.125\ k_o$	132	6.4	20.31
20	$-.125\ k_o$ to $+.125\ k_o$	88	5.1	17.25
20	$-.0625\ k_o$ to $+.0625\ k_o$	88	2.8	31.43

CHAPTER V

CONCLUSIONS AND RECOMMENDATIONS

The preceding chapters have discussed the application of plane wave spectrum analysis techniques to the determination of near-zone radiated fields. A technique has been outlined which permits these patterns to be determined to a specified angular resolution by using a numerical interpolation and a technique for minimizing the computation time required to demonstrate the antenna near-zone fields by using a wave-band filter has also been presented. This technique has direct application to radiation hazard analysis where the antenna near-zone fields must be determined over wide angular sectors.

The plane wave spectrum representation offers an approach which compliments the Green's function approach. It is concluded that the advantage of this technique is greatest for large apertures at relatively close-in near-field ranges. This is due to the fact that the computation time increases approximately linearly with aperture size for the PWS method; whereas, the aperture field integration method increases with the square of the aperture dimension. It is also concluded from these studies that in order to describe a particular near-field region, integration over all visible wavenumbers is not necessary. A relation defining the size of the spectral region required to accurately determine the significant near-field contributions in a particular region and the angular location of that region has been derived which results in

significantly reduced computation times. This further reduction is proportional to the square of the ratio of the number of filtered spectral samples to unfiltered samples along a linear dimension of a square array of spectral data.

These techniques are also useful for application to near-field scattering problems. However, the form of the integrand is more complicated in that case due to the presence of the obstacle scattering coefficients. It is recommended that further study of the application of these bandpass filtering techniques to the complex integrand for near-field scattering analysis be performed.

A P P E N D I X

APPENDIX

INTEGRATION FORMULA BASED ON BIVARIATE INTERPOLATION OF THE INTEGRAND

Consider an integrand I of the form

$$I = \int_{v_1}^{v_2} \int_{u_1}^{u_2} f(u, v)\, e^{j(au + bv)}\, du\, dv \qquad \text{(A1)}$$

where the integration is performed on the square patch shown in Figure 34. If the function f(u, v) is defined at the corners of the patch, the function within the patch can be approximated by the 4-point bivariate interpolation formula [33].

$$f(u_0 + pg,\ v_0 + qh) = (1-p)(1-q)f_{00} + p(1-q)f_{10} + q(1-p)f_{01} + pq\, f_{11}\ , \qquad \text{(A2)}$$

where,

$$f_{00} = f(u_o,\ v_o)\ ,$$
$$f_{01} = f(u_o, v_o + h)\ ,$$
$$f_{10} = f(u_o + g,\ v_o),\ \text{and}$$
$$f_{11} = f(u_o + g,\ v_o + h)\ .$$

Thus, the integral I_i on the i'th patch takes the form,

$$I_i = \int_{q=0}^{1} \int_{p=0}^{1} f(p,q)\, e^{ja(u_o + pg)}\, e^{jb(v_o + qh)}\, [(gh)\, dp\, dq]\ . \qquad \text{(A3)}$$

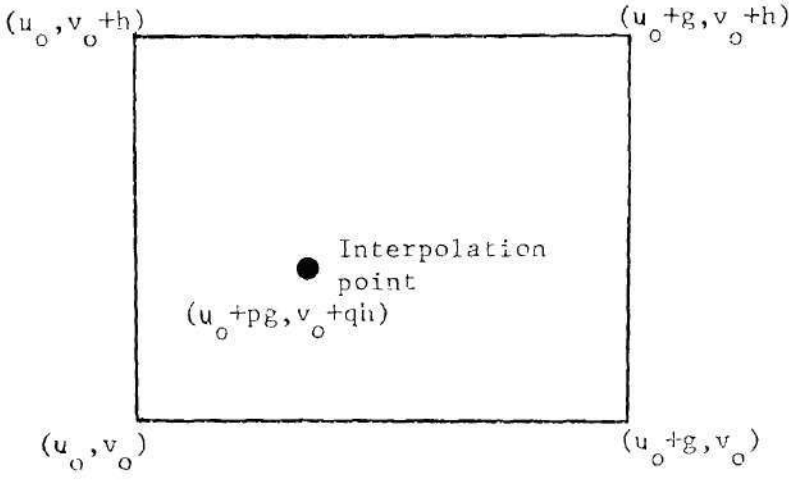

Figure 34. Geometry of the Surface Patch Used in the Bivariate Interpolation Integration Formula.

Using the interpolation formula given in equation (A2), this integral can be expressed as the sum of four integrals as

$$I_i = (gh)\, e^{j(au_o + bv_o)} \{ f_{00} I_{i,1} + (f_{10} - f_{00}) I_{i,2} + (f_{01} - f_{00})\, I_{i,3} + (f_{00} - f_{01} - f_{10} + f_{11})\, I_{i,4} \}, \tag{A4}$$

where the integrals $I_{i,j}$ are given by

$$I_{i,1} = \int_{q=0}^{1} \int_{p=0}^{1} e^{jagp} e^{jbhq}\, dpdq ,$$

$$I_{i,2} = \int_{q=0}^{1} \int_{p=0}^{1} p\, e^{jagp} e^{jbhq}\, dpdq ,$$

$$I_{i,3} = \int_{q=0}^{1} \int_{p=0}^{1} q\, e^{jagp} e^{jbhq}\, dpdq , \quad \text{and}$$

$$I_{i,4} = \int_{q=0}^{1} \int_{p=0}^{1} p\, q\, e^{jagp} e^{jbhq}\, dpdq .$$

These integrals are evaluated in closed form as

$$I_{i,1} = [\frac{1}{jag} (e^{jag} - 1)][\frac{1}{jbh} (e^{jbh} - 1)] ,$$

$$I_{i,2} = - \frac{1}{(ag)^2} [e^{jag}(jag - 1) - 1][\frac{1}{jbh} (e^{jbh} - 1)] , \tag{A5}$$

(continued)

$$I_{i,3} = -\frac{1}{(bh)^2}\left[e^{jbh}\,(jbh - 1) - 1\right]\left[\frac{1}{jag}\,(e^{jag} - 1)\right], \text{ and}$$

$$I_{i,4} = \frac{1}{(ag)} \cdot (bh)^2\left[e^{jag}(jag - 1) - 1\right]\left[e^{jbh}(jbh - 1) - 1\right].$$

These closed form expressions can be easily implemented in a computer algorithm and are a two-dimensional form of the linear Filon Quadrature formula [33].

When these formulas are used to evaluate a given integrand f(u,v) the patch size must be chosen such that the bivariate interpolation formula gives a good approximation to the function over the integration patch. An integration over a large area can then be performed by using a grid of patches which covers the entire integration area. Formulas of this type have been found to be more accurate than the trapezoidal integration rule for the evaluation of radiation integrals.

BIBLIOGRAPHY

1. Silver, S., Microwave Antenna Theory and Design, Chapter 5 and 6, McGraw Hill, New York, 1949.

2. Hansen, R. C., Microwave Scanning Antennas, Vol. 1, Academic Press, New York, 1964, pp. 21-46.

3. Bouwkamp, C. J., "Diffraction Theory," Rep. Progr. Phys., Vol. 17, 1954, pp. 35-100.

4. Hansen, R. C., and Bailin, L. L., "A New Method for Near Field Analysis," IRE Trans. Antennas Propagation, Vol. AP-17, 1959, pp. S458-S467.

5. Walter, C. H., Traveling Wave Antennas, McGraw-Hill, New York, 1965, pp. 49-62.

6. Jacobs, E., "Predicting Power Transfer Between Large Aperture Antennas At Close Separations," IRE Trans. Radio Freq. Interference, 1962, pp. 23-40.

7. Booker, H. G. and Clemmow, P. C., "The Concept of an Angular Spectrum of Plane Waves," J. Inst. Elec. Eng., Vol. 97, 1950, pp. 11-17.

8. Brown, J., "Theoretical Analysis of Some Errors in Aerial Measurements," J. Inst. Elec. Eng., Vol. 105 (part C), February 1958, pp. 343-351.

9. Clemmow, P. C., The Plane Wave Spectrum Representation of Electromagnetic Fields, Pergamon Press, New York, 1966.

10. Joy, E. G. and Paris, D. T., "Spatial Sampling and Filtering in Near-Field Measurements," IEEE Trans. Antennas Propagation, Vol. AP-20, 1972, pp. 253-261.

11. Leach, W. M. and Paris, D. T., "Probe Compensated Near-Field Measurements on a Cylinder," IEEE Trans. Antennas Propagation, Vol. AP-21, No. 4, July 1973, pp. 435-445.

12. Rodrigue, G. P., Joy, E. B., and Burns, C. P., "An Investigation of the Accuracy of Far-Field Radiation Patterns Determined from Near-Field Measurements," Final Report on U. S. Army Missile Command, Contract DAAH01-72-C-0950, August 1973.

13. Joy, E. B., Burns, C. P., Rodrigue, G. P., and Burdette, E. C., "Accuracy of Hemispherical Far-Field Patterns Determined from Near-Field Measurements," 1975 AP-S Symposium, Urbana, Illinois, June 1975.

14. Rodrigue, G. P., Joy, E. B., Huddleston, G. K., Burns, C. P., and Burdette, E. C., "A Study of Phased Array Antenna Patterns Determined by Measurements on a Near-Field Range," Final Engineering Report, Georgia Institute of Technology, March 1975.

15. Ecker, H. A., Burns, C. P., Hightower, N. C., Burdette, E. C., Evans, J. L. and Riherd, F. T., "Automated Near-Field Measurements to Obtain Far-Field Patterns of Aperture Antennas and Phased Arrays," 1974 International IEEE/AP-S Symposium, June 10-12, 1974, pp. 161-164.

16. Baird, R. C., Newell, A. C., Wacker, P. F., and Kerns, D. M., "Recent Experimental Results in Near-Field Antenna Measurements," Electron. Lett., Vol. 6, pp. 347, May, 1970.

17. Leach, W. M., Joy, E. B., and Paris, D. T., "Probe Compensated Near-Field Measurements: Basic Theory, Numerical Techniques, Accuracy," Presented at the 1974 International IEEE AP-S/URSI Symposium, June, 1974.

18. Johnson, R. C., Ecker, H. A., and Hollis, J. S., "Determination of Far-Field Antenna Patterns from Near-Field Measurements," IEEE Proceedings, Vol. 61, No. 12, pp. 1668-1694, 1973.

19. Rudduck, R. C., Wu, D. C. F., and Intihar, M. R., "Near-Field Analysis by the Plane Wave Spectrum Approach," IEEE Trans. Antennas Propagation, AP-21, No. 2, pp. 231-234, 1973.

20. Rhodes, D. R., "On a Fundamental Principle in the Theory of Planar Antennas," IEEE Proceedings, Vol. 52, pp. 1013-1021, 1964.

21. Brown, A. C., Jr., "Antenna Near Field Pattern Computation by Plane Wave Spectrum Integration," 1975 USNC/URSI Meeting Abstracts, June 1975, p. 79.

22. "Special Issue on Rays and Beams," Proc. IEEE Vol. 62, No. 11, November 1974.

23. Kerns, D. M., "Correction of Near-Field Antenna Measurements Made with an Arbitrary but Known Measuring Antenna," Electron. Lett., Vol. 6, 1970, pp. 346-347.

24. Paris, D. T., "Digital Computer Analysis of Aperture Antennas," IEEE Trans. Antennas Propagation, Vol. AP-16, March 1968, pp. 262-264.

25. Deschamps, G. A., "Ray Techniques in Electromagnetics," IEEE Proceedings Vol. 60, No. 9, pp. 1022-1035, September 1972.

26. Sommerfeld, A., Optics, Volume IV, "Lectures on Theoretical Physics," New York, Academic Press, 1964.

27. Luneberg, R. K., Mathematical Theory of Optics, Berkeley and Los Angeles, California: Univ. Calif. Press, 1964.

28. Choudhary, S. and Felsen, L. B., "Analysis of Gaussian Beam Propagation and Diffraction by Inhomogeneous Wave Tracking," Proceedings of the IEEE, Vol. 62, No. 11, pp. 1530-1541, November 1974.

29. Kramers, H. A., Quantum Mechanics, Dover Publications, New York, 1964, pp. 14-28.

30. Messiah, A., Quantum Mechanics, Volume I, North-Holland Publishing Company, Amsterdam, 1961.

31. Papoulis, A., The Fourier Integral and Its Applications, McGraw-Hill Book Company, 1962, pp. 62-74.

32. Ryan, C. E. and Cain, F. L., Polar Pattern Near-Field Test Measurements of Agiltrack Phased Array Antenna, Private Communication, 1976.

33. Abramowitz, M. and Stegun, I. A., Handbook of Mathematical Functions, National Bureau of Standards, Applied Mathematics Series-55, 1964.

34. Richmond, J. H., "A Wire-Grid Model for Scattering by Conducting Bodies," IEEE-T-AP Vol. 15, November 1967, p. 802.